DERIVATION OF SEISMIC DESIGN PARAMETERS FOR HIGH-PERFORMANCE FIBER REINFORCED CONCRETE (HPFRC) AND MULTI-MATERIAL BUILDINGS

A Thesis

Presented to

the Faculty of the Department of Civil and Environmental Engineering

University of Houston

In Partial Fulfillment

of the Requirements for the Degree

Master of Science

in Civil Engineering

by

Ibrahim KAYMAZ

December 2013

DERIVATION OF SEISMIC DESIGN PARAMETERS FOR HIGH-PERFORMANCE FIBER REINFORCED CONCRETE (HPFRC) AND MULTI-MATERIAL BUILDINGS

Ibrahim KAYMAZ

Approved:

Chair of the Committee
Bora Gencturk, Assistant Professor,
Civil and Environmental Engineering

Committee Members:

Abdeldjelil Belarbi, Professor,
Civil and Environmental Engineering

Haleh Ardebili, Assistant Professor,
Mechanical Engineering

Bora Gencturk, Assistant Professor,
Civil and Environmental Engineering

Suresh K. Khator, Associate Dean,
Cullen College of Engineering

Kaspar J Willam, Professor,
Department Chair

Acknowledgement

I would like to express my sincere gratitude to my advisor Dr. Bora Gencturk for his continuous support, his patience, motivation, and immense knowledge. He patiently encouraged and advised me to proceed and complete my thesis. I could not have imagined having a better advisor and mentor for my thesis.

I would like to thank my rest of the committee members, Dr. Abdeldjelil Belarbi and Dr. Haleh Ardebili for their evaluations and insightful comments. I would like to thank Turkish Pipeline Petroleum Company for their financial support during my study. In addition, I would like to thank also my group mates in Sustainable and Resilient Structures Group. I do appreciate their endless help and support during my MSCE.

Last but not the least, I would like to thank my parents, my brother, and my sisters for their support. Finally, I especially thank to my wife, Hicran, and my son, Omer Alper, for their endless support and patience.

DERIVATION OF SEISMIC DESIGN PARAMETERS FOR HIGH-PERFORMANCE FIBER REINFORCED CONCRETE (HPFRC) AND MULTI-MATERIAL BUILDINGS

An Abstract

of a

Thesis

Presented to

the Faculty of the Department of Civil and Environmental Engineering

University of Houston

In Partial Fulfillment

of the Requirements for the Degree

Master of Science

in Civil Engineering

by

Ibrahim KAYMAZ

December 2013

ABSTRACT

Over the past decade, various experimental studies have demonstrated the advantages of high-performance fiber reinforced concrete (HPFRC) for seismic applications, most importantly high ductility, energy absorption capacity and damage tolerance. However, large-scale applications of HPFRC are still rare today, mainly resulting from two facts: lack of explicit design guidelines and high cost. In this study, seismic design parameters; namely, response modification, system overstrength and displacement amplification factors *(R, Ω_0, C_d)* are derived for reinforced concrete moment resisting frames based on the procedure outlined in FEMA P695. Two different buildings designs are considered. In one of these designs, the concrete is entirely replaced with HPFRC. In the second design, to address the cost issue, only the plastic hinge regions are built from HPFRC while reinforced concrete is used for the rest of the buildings. The seismic design factors are quantified using the current code concepts, with the help of incremental dynamic analyses and finally by means of risk assessment techniques. The results are proposed as a basis for further research on seismic design of HPFRC and multi-material buildings.

Table of Content

List of Figures

List of Tables

List of Symbols

A_g = gross cross-sectional area of an element

a = material constant for steel model

b = element width

b = material constant for steel model

C = constant which is a function of the building's natural period (ATC-19, 1995).

C_d = deflection amplification factor (Table 12.2-1 of ASCE/SEI 7-05)

C_s = seismic response coefficient (Section 12.8.1.1 of ASCE/SEI 7-05)

C_t = approximate period coefficient (Table 12.8-2 of ASCE/SEI 7-05)

C_u = upper-limit period coefficient (Table 12.8-1 of ASCE/SEI 7-05)

d = column depth

D = dead load

E = Young's modulus

EI_g = gross cross-sectional moment of inertia

E_t = total energy dissipation capacity

E_D = energy loss off frame under cyclic analysis

E_{S0} = maximum strain energy

F_a = short-period site coefficient (Section 11.4.3 of ASCE/SEI 7-05)

F_v = long-period site coefficient (Section 11.4.3 of ASCE/SEI 7-05)

F_y = yield strength of material

fc = compressive strength of unconfined concrete,

f_y = yield stress of longitudinal reinforcement

g = constant acceleration due to gravity

h = element height

I = importance factor (Section 11.5.1 of ASCE/SEI 7-05)

K = horizontal force factor

L = live load

N = number of levels (stories) in an index archetype model

n = material constant for steel model

P = axial load

Q_E = the effect of horizontal seismic force from total design base shear, V,

R = response modification coefficient (Table 12.2-1 of ASCE/SEI 7-05)

R_s = period dependent strength factor

R_μ = period dependent ductility factor

R_R = redundancy factor.

s = spacing of transverse reinforcement in the column hinge region

S = snow load

S_1 = mapped MCE, 5-percent damped, spectral response acceleration parameter at a period of 1 second as defined in Section 11.4.1 of ASCE/SEI 7-05

$\hat{S}_{CT}$ = median value of collapse level earthquake, 5-percent damped, spectral response acceleration at the fundamental period, T, of the building (Site Class D)

S_{DS} = design, 5-percent damped, spectral response acceleration parameter at short periods as defined in Section 11.4.4 of ASCE/SEI 7-05

S_{D1} = design, 5-percent damped, spectral response acceleration parameter at a period of 1 second as defined in Section 11.4.4 of ASCE/SEI 7-05

S_{MS} = the MCE, 5-percent damped, spectral response acceleration parameter at short periods adjusted for site class effects as defined in Section 11.4.3 of ASCE/SEI 7-05

S_{MT} = MCE, 5-percent damped, spectral response acceleration at the fundamental period, T, of the building, as defined in Section 11.4.3 of ASCE/SEI 7-05 (Site Class D)

S_{M1} = the MCE, 5-percent damped, spectral response acceleration parameter at a period of 1 second adjusted for site class effects as defined in Section 11.4.3 of ASCE/SEI 7-05 (Site Class D)

S_S = mapped MCE, 5-percent damped, spectral response acceleration parameter at short periods as defined in Section 11.4.1 of ASCE/SEI 7-05

S_T = median value of normalized record set, 5-percent damped, spectral response acceleration at the fundamental period, T

S_a = spectra acceleration, g

$S_a(T)$ = the spectral acceleration at the period, T

SF = record (and component) scale factor required for collapse evaluation of an individual building

T = the fundamental period of the building,

T_1 = the fundamental period of the building determined by eigenvalue analysis

T_a = the approximate fundamental period of the building

T_s = short-period transition period of the building

V_d = design base shear

V_e = elastic base shear

V_{max} = maximum base shear

W = effective seismic weight of the building

Z = seismic zone factor

x = parameter (Table 12.8-2 of ASCE/SEI 7 -05)

β_{DR} = design requirements-related collapse uncertainty

β_I = component of effective damping of the structure

β_{MDL} = modeling-related collapse uncertainty

β_{RTR} = record-to-record collapse uncertainty

β_{TD} = test data-related collapse uncertainty

β_{TOT} = total system collapse uncertainty

ε_{t0} = first cracking strain

ε_{tp} = strain at peak stress in tension

ε_{tu} = tensile strain capacity

ε_{cp} = strain at peak stress in compression

ε_{cu} = ultimate strain in compression

σ_{tp} = strength in tension

σ_{cp} = strength in compression

σ_{cr} = stress on the compression envelope corresponding ε_{cu}

δ = roof drift

δ_u = ultimate roof displacement

$\delta_{y,eff}$ = effective roof displacement

μ_T = period-based ductility

ρ = ratio of total area of longitudinal reinforcement

ρ' = ratio compressive longitudinal reinforcement of beams

ρ_{sh} = area ratio of transverse reinforcement in column hinge region

Ω = calculated overstrength of an index archetype analysis model

Ω_O = system overstrength factor (Table 12.2-1 of ASCE/SEI 7-05)

ξ = damping factor

List of Abbreviations

ACMR = adjusted collapse margin ratio

ACI = American Concrete Institute

ATC = Applied Technology Council

ASCE = American Society of Civil Engineers

ASTM = American Society for Testing and Materials

BOCA = Building Officials Code Administrators International

CMR = collapse margin ratio

DE = design earthquake

DMs = damages measures

DR = design requirements uncertainty

ECC = Engineered Cementitious Composites

ELF = equivalent lateral force

FEMA = Federal Emergency Management Agency

HPFRC = High-Performance Fiber-Reinforced Concrete

IBC = International Building Code

ICC = International Code Council

ICBO = International Conference of Building Officials

IDA = incremental dynamic analysis

IMs = intensity measures

MAE Center = Mid-America Earthquake Center

MCE = maximum considered earthquake

MDL = model quality uncertainty

MX = mixed design of RC and ECC

NCEER = National Center for Earthquake Engineering Research

NGA = Next generation attenuation

NSF = National Science Foundation

P = perimeter frame system

PEER = Pacific Earthquake Research Center

PG = performance group

PGA = peak ground acceleration

PGV = peak ground velocity

RC = reinforced concrete

RSA = response spectrum analysis

RTR = record-to-record uncertainty

R/ECC = reinforced engineered cementitious composites

S = space frame system

SBCCI = Southern Building Code Congress International

SCWB = strong-column weak-beam

SDC = seismic design category

SEAOC = Structural Engineers Association of California

SMRF = special moment resisting frame

SPFs = seismic performance factors

SSF = spectral shape factor

TD = test data uncertainty

Chapter 1 Introduction

1.1 Background

In parallel with the technological, social and economic developments, the requirements for the design and construction of civil structures have changed in many ways. Researchers and engineers have started to investigate sustainable and innovative structural materials to meet the increases in social and economic demands. At the same time, recent earthquakes have demonstrated that, as engineers, we still lack a complete understanding of the performance of structures when subjected to complex dynamic loading. Researchers and engineers are now spending more effort to reduce the effects of earthquake during the service life of structures encouraged by the substantial improvements in the mechanical and durability performance of construction materials in the recent years.

Engineered Cementitious Composites (ECC), which is a special type of High-Performance Fiber-Reinforced Concrete (HPFRC), designed based on micromechanical principles (Li 1992b, Li and Leung 1992, Li and Wu 1992, Li 1992a) is one of these materials. ECC has superior damage tolerance and shear resistance, reduced crack widths, and high energy dissipation compared to conventional concrete (Fukuyama et al. 2000, Billington and Yoon 2004, Kanda, Watanabe, and Li 1998, Fischer and Li 2002). The material and component level tests that have demonstrated the advantages of ECC and other types of HPFRC have not resulted in widespread implementation at the system level. The main reasons for underutilization of ECC in real life applications are the high cost and lack of comprehensive seismic design guidelines for such materials. Therefore, there is a need to derive seismic performance factors (SPFs), namely response

modification (R), system overstrength (Ω_0), and deflection amplification (C_d) factors at the minimum, for structures utilizing ECC as a construction material.

In order to prevent the loss of lives besides economic losses, code regulations are considered as essential. In 2004, Federal Emergency Management Agency (FEMA) started a project with the Applied Technology Council (ATC) to develop a methodology, which is applicable to all type of structures, for calculating, standardized design parameters. The new methodology developed by the ATC-63 Project is primarily based on the "Tentative Provisions for the Development of Seismic Regulations for Buildings, ATC-3 06" (ATC 1978) and the "Recommended Provisions for Seismic Regulations for New Buildings and Other Structures, 2003" (FEMA 2003). The developed methodology has been applied to certain types of structures such as steel, conventional concrete and timber, to derive or validate seismic design parameters for the code regulations. However, no such study has been conducted for buildings using HPFRC and thus the seismic design parameters are still unknown for these special structures.

1.2 Objectives and Scope

ECC are being more and more used in structures, but there are still no established seismic design parameters of these structures. The main objective of this thesis is to address this issues by developing seismic design parameters for buildings that use ECC following the FEMA P695 (FEMA 2009) methodology. Specifically, response modification (R), system overstrength (Ω_0), and deflection amplification (C_d) factors are derived for special moment resisting frames (SMRF). These frames are called "special" due to their performance under strong earthquakes. They exhibit large inelastic displacements without collapse because of well detailed beams, columns and beam-

column connections comparison to the ordinary moment resisting frames. For this purpose, three building designs were considered in this thesis. The cost of ECC might be 4-5 times of the cost of the conventional concrete depending on the selection of the mixture materials and fibers. Therefore, to use the material in an innovative and cost effective manner, in one of the designs, ECC is used only in the plastic hinge regions of the buildings while RC is used for the rest. These buildings are referred to as MX frames in the remainder of this thesis. The other two designs use either entirely reinforced ECC or entirely RC. The MX frame is illustrated in Figure 1-1.

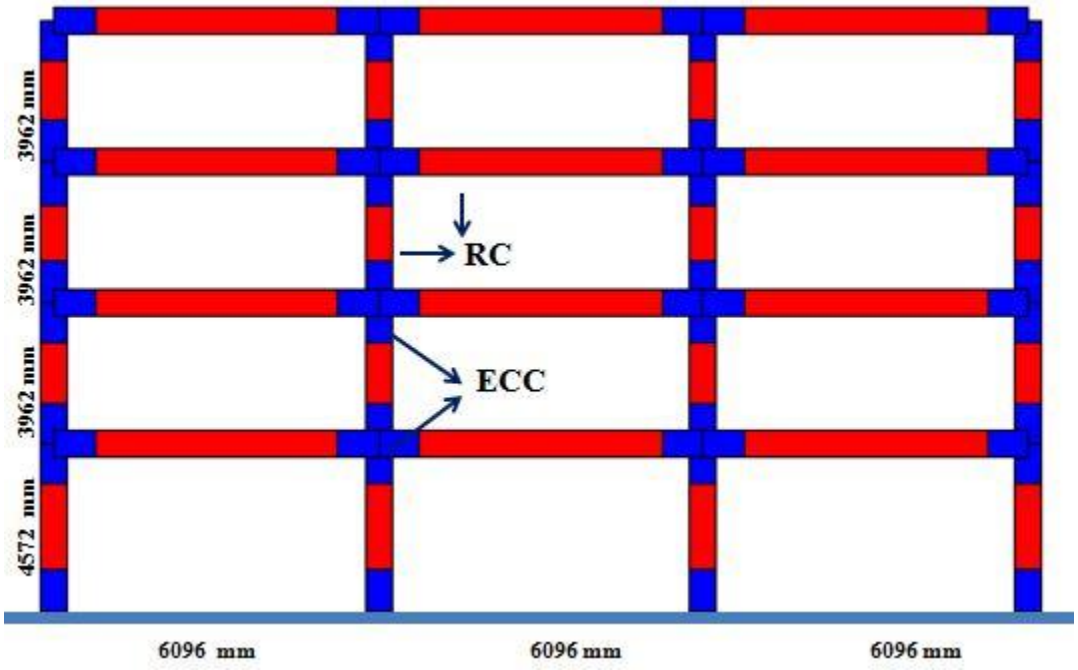

Figure 1-1 Example four-story MX frame.

1.3 Research Approach

The methodology for the derivation of seismic design parameters progresses following these steps: gathering the required information on design requirements and materials, development of analytical models, analysis of models and evaluation of the data from incremental dynamic analysis. Based on the FEMA P695 (FEMA 2009)

methodology, data for design of the models were collected from the seismic design codes and standards and also material properties were determined for concrete, steel and ECC. The archetypes were modeled as R/ECC, RC and MX frames. The frames were analyzed using both nonlinear static and dynamic analysis for collapse performance. Finally, the collapse results of models were assessed to obtain the seismic design parameters.

1.4 Content and Organization

This thesis is divided into chapters, and organized as follows:

Chapter 2 covers the literature review of studies on seismic design parameters and beam-column joints for both reinforced ECC (R/ECC) and reinforced concrete structures (RC).

Chapter 3 provides a detailed description of FEMA P695 methodology since it is essential to the work performed here.

Chapter 4 describes the archetype development procedure which includes materials, loads, and frame types and configurations.

Chapter 5 presents the results from the nonlinear analysis of archetypes for the collapse assessment procedure.

Chapter 6 evaluates the results from Chapter 5 and derives the seismic design parameters based on FEMA P695 performance evaluation criteria.

Chapter 7 provides conclusions, limitations, and suggestions for future research.

Appendix-A provides the nonlinear static analysis results.

Chapter 2 Literature Review

2.1 Introduction

The collapse limits for structures are one of the key parameters in derivation of seismic design parameters. In parallel with the developments in seismic design provisions for structural systems designed with different type of materials, understanding the effects of seismic design parameters on the collapse behavior started to attract more attention from the research community. Previous studies show that beam column joints are crucial parts of RC moment resisting frames due to their influence on the collapse behavior (Leon 1990, Walker 2001, Altoontash and Deierlein 2004). In this study the behavior of R/ECC and MX buildings, both of which use ECC material in the shear panel zone and plastic hinges, are investigated. Therefore, in the absence of prior studies on derivation of seismic design parameters for building using HPFRC, the literature review in this thesis mainly focuses on the behavior of beam-column joints in RC structures.

2.2 Previous Studies on Beam Column Joints

Beam-column joints are an integral part of moment resisting frames whose key behavior features such as energy dissipation capacity determines the overall structural performance (Park and Ruitong 1988, Shiohara 2004, Somma, 2011). In ACI 352-R02 (2002) joints are defined as “portion of the column within the depth of the deepest beam that frames into the column.” Their functional requirement is to enable the adjoining members to develop and sustain their ultimate capacity under seismic loads (Kavitha and Damodarasamy 2009). Figure 2-1 is a general visualization of beam-column joints for reinforced concrete structures.

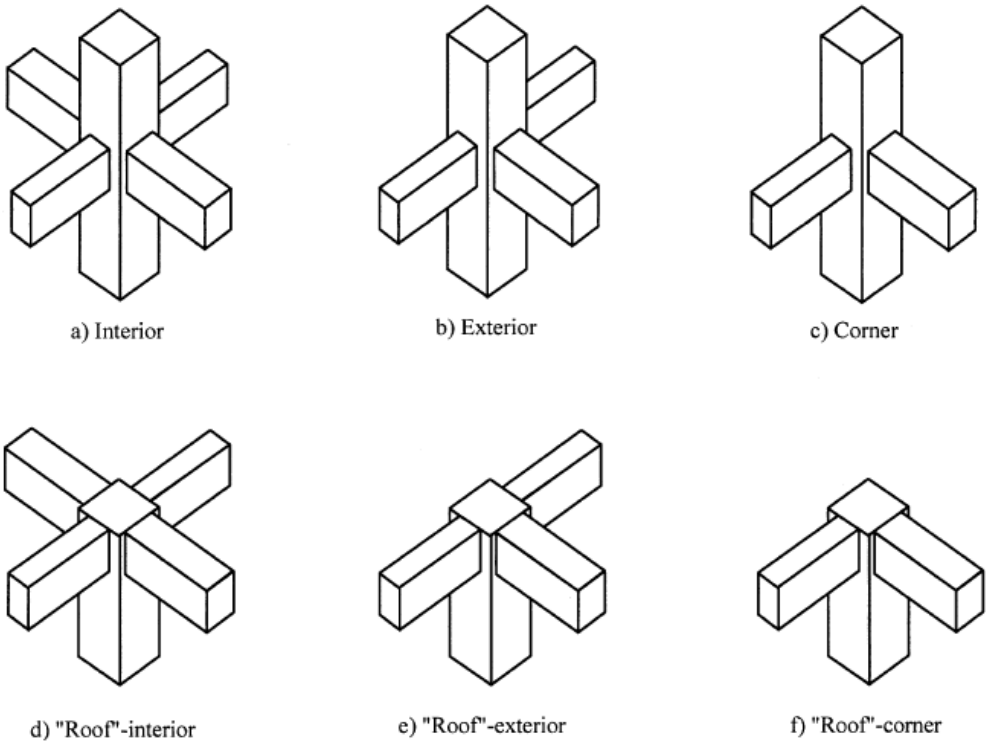

Figure 2-1 Typical beam-to-column connections (ACI 2002).

2.2.1 Experimental Studies on Reinforced Concrete Beam Column Joints

Due to their complex geometry and variability in material properties, there are several factors which are influential on the behavior of RC beam-column joints. A large number of studies investigated the joint behavior either experimentally or analytically. Regarding the prior experimental work, researchers first investigated main parameters such as the joint shear behavior, joint core confinement, concrete compressive strength, bond resistance and axial load level which control the joint response and concluded that the overall joint performance is affected by the shear forces from the beams and columns and also from the flexural behavior of the adjoining members. While horizontal shear resistance is provided by the transverse reinforcement, the vertical shear resistance is provided by the longitudinal reinforcement.

One of the first experimental studies conducted by Higashi and Ohwada (1969) concluded that joint shear demand is an important parameter to define the failure mode. Meinheit and Jirsa (1977) also concluded that joint shear strength has a significant influence on the joint behavior and increases with increasing area of column longitudinal reinforcement. Confinement of the joint core was found to be the second most influential parameter. Durrani and Wight (1982) who conducted an experimental program concluded that increasing the amount of hoop steel reinforcement in the joint region lowers the joint shear stress demand and prevents the brittle joint failure by providing more ductility. Two years later Otani et al. (1984) reached the same conclusion. Similarly, the study of Noguchi and Kashiwazaki (1992) showed that confinement plays an important role on ductility, especially after large deformations . Kaku and Asakusa (1991) also observed that the ductility of the specimens increased with increasing joint hoop reinforcement.

Concrete compressive strength is a factor that contributes to the bond resistance and shear strength of the joint. Endoh et al. (1991) concluded that the reduced concrete compressive strength decreases the shear strength. Oka and Shiohara (1992) also obtained similar results and formulated a relationship between compressive strength and joint shear capacity. There are regulations provided in ACI 352R-02 (2002) for minimum and maximum reinforcement ratio and spacing of transverse reinforcement to provide enough ductility under earthquake loads. Bond resistance is another important factor for beam column joint response under earthquake loading. If the bond resistance is weak then strength deterioration should be expected, which might result in the slippage of the longitudinal reinforcement from the joint region. The bond resistance of rebar in joints is

also function of the development length, and shear resistance and confinement of the joint region. The stronger the bond between concrete and reinforcement, the more the energy dissipation is. It was also shown by Brooke et al. (2004) that the bond performance increases with increasing vertical reinforcement in the joint region, and the design drift limit is related to the bond resistance. Kaku and Asakusa (1991) examined the effect of axial load level and they observed that the joint shear strength increases with increasing axial load. Furthermore, they concluded that the axial load increases the ductility of the members and the energy dissipation capacity. Meinheit and Jirsa (1977) concluded that the column axial load influences the shear cracking stress and the inclination of the shear cracks in the joint region. Park and Ruitong (1988) tested four interior joints and concluded that if the column interior bars transmit the shear force through the joint region then low axial load ratio should be expected. The test results of Clyde et al. (2000) showed that the increasing axial load level increases the joint shear strength and energy dissipation. Earlier experimental studies concur on the effects of transverse reinforcement and axial load, and emphasize the complexity of load transfer mechanisms in the joints.

2.2.2 Experimental Studies on ECC Beam Column Joints

Since the introduction of HPFRC, numbers of experimental studies were conducted on the use of HPFRC in beam-column joints. Experimental studies proved that the use of HPFRC, either at the plastic hinge region or at the beam-column joint region improves the performance of the structure under earthquake loads. One of the earliest test program conducted by Henager (1977) on investigation of the beam-column joint regions constructed with steel fiber reinforced concrete. After testing two exterior beam-column

joints with and without steel fibers under reverse cyclic loading; the test for specimen constructed with steel fibers resulted higher energy dissipation, higher damage tolerance and less strength deterioration. The study of Filiatrault et al. (1994) showed that depend on the volume of fibers used in beam-column joint region influence the final behavior of the structure. The specimens with steel fibers increased the shear resistance and the failure mode was changed from joint shear failure to beam plastic hinge failure besides increasing energy dissipation and ductility. One year later, they also tested three interior beam-column joints to investigate the effect of steel fiber. The specimen with steel fiber performed well and resulted with higher shear strength, higher energy dissipation and adequate ductility (Filiatrault, Pineau, and Houde 1995). Test program of Katzensteiner et al. (1992) was on investigation of using high performance materials at in the joint region of two-bay two story frame. They used steel fibers in the joint regions. The frame with the high performance material performed well and resulted around 1.4 times more energy dissipation. In the same year, Jiuru et al. (1992) test program with both interior and exterior beam-column joints resulted in favor of HPFRC. The specimens with steel fibers improved the joint shear strength and reduced the bar slippage. In 2000, Parra-Montesinos and Wight (2000) investigated result of replacement of joint transverse reinforcement with ECC in exterior joints. The specimen with ECC performed well under loads. Both better shear response and reduced crack width with less damage observed after the test program. Another test program conducted by Gebman (2001) on beam-column joints resulted that the energy dissipation capacity of specimens with high performance materials was 1.0 to 3.0 times higher than the conventional concrete joints, and damage tolerance improved besides higher load carrying capacity. Fisher and Li

(2002) found that the energy dissipation capacity of steel reinforced ECC members are significantly higher compared to that of conventional concrete members. Additionally, the study of Billington and Yoon (2004) on precast concrete bridge pier systems concluded that the use of ductile fiber-reinforced cementitious composites (DFRCC) at the plastic hinge regions of columns increases the energy dissipation capacity. Moreover, spalling of cover concrete was not observed for DFRCC even at large displacements. Canbolat et al. (2005) investigated the use of high-performance fiber-reinforced cementitious composites (HPFRCC) in coupling beams with a simplified reinforcement detailing. Major conclusions from that study were that HPFRCC specimens exhibited higher shear stress and stiffness retention, superior damage tolerance under large displacements and same seismic performance with a simplified reinforcement detailing. Shannag et al. (2005) Beam-column joint test used high performance steel fiber reinforced concrete at the beam-column joint regions. The results indicated that use of steel fiber concrete yields higher ductility and joint strength, three times more load carrying capacity, and 20 times more energy dissipation. Pan and Yuan (2013) investigated the seismic behavior of ECC and concrete composite beam-column joints under reversed cyclic loading. Observations were in agreement with those of other researchers that "the composite beam-column joints showed higher load capacity, ductility and energy dissipation when compared with RC beam-column joint specimen." In the light of these findings, the idea of substituting conventional concrete with ECC in beam column joint regions can significantly increase the seismic performance of structures under earthquake loads.

2.2.3 Analytical Studies

In parallel with experimental studies on beam column joints, researchers also performed analytical modeling of beam-column joints to predict the effects of different parameters and overall of response of structures. Giberson (1969) develop a one component frame model which consists of a beam element with two nonlinear rotational springs attached to the end of the member as shown in Figure 2-2. This model was not able to capture the actual moment rotation behavior of the element by using predefined moment values. A more developed version of this model was proposed by Otani (1974) as a two component frame model with two parallel line elements and two rigid line elements shown in Figure 2-3. The joint panel was assumed fully rigid and the rotational springs were representing the member end rotation out of joint core. The shear deformations were neglected.

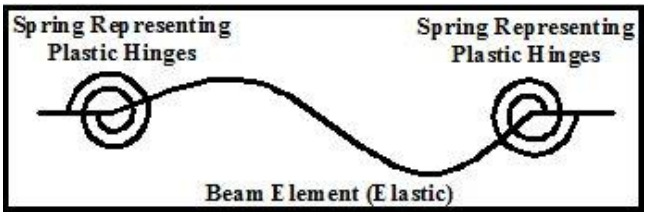

Figure 2-2 Giberson one-component model (Giberson 1969).

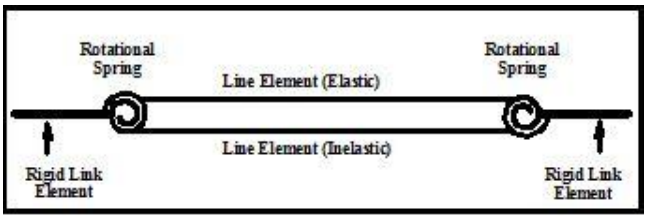

Figure 2-3 Otani two-component model (Otani 1974).

Later on, Anderson and Townsend (1977) improved the two component frame model by Otani (1974) by adding the joint shear deformation effect. Another model was developed by El-Metwally and Chen (1988) by putting a zero length rotational spring at

the beam-column joint region. They were able to capture the initial stiffness, maximum moment carrying capacity and energy dissipation; however, strength and stiffness deterioration could be predicted well with this model. Definition of the panel zone is one of the main challenges of beam-column joint modeling. Alath and Kunnath (1995) proposed a model called the "panel zone model" by adding rigid link elements to the end of the members with one inelastic rotational spring as shown in Figure 2-4. While this model was capable of representing the shear behavior of the panel zone using an empirical relationship, the bar slips behavior of the members was not considered. Four years later, Biddah and Ghobarah (1999) proposed a model considering the bar slip behavior by adding one more spring to the joint model.

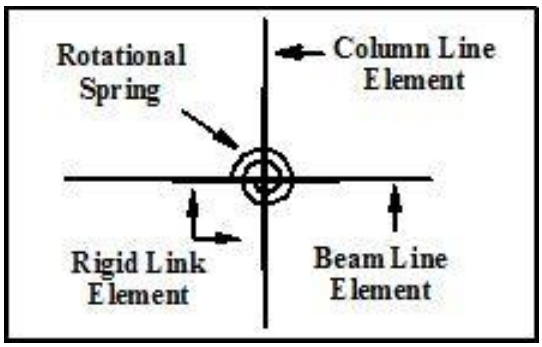

Figure 2-4 Panel zone model of Alath and Kunnah (1995).

A more complex model was proposed by Elmorsi et al. (2000) using a joint panel region element and transition elements, representing the beam-column plastic hinge region. The joint element was connected to transition element and transition element was connected to elastic line elements representing the beams and the columns. This model was capable of modeling behavior of concrete and reinforcing bars, in addition to the interaction between the two. The details of this model are shown in Figure 2-5.

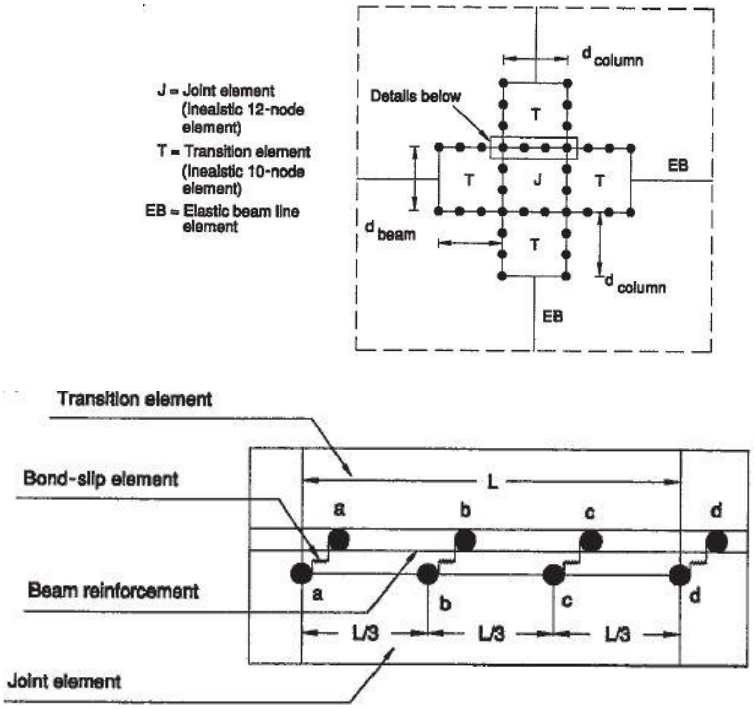

Figure 2-5 Beam-column joint model of Elmorsi et al. (2000).

The joint model by consisted of two diagonal translational springs in the joint panel zone for the shear behavior and 12 additional springs for bond slip and concrete crushing. The model proposed by Youssef and Ghobarah (2001) is shown in Figure 2-6.

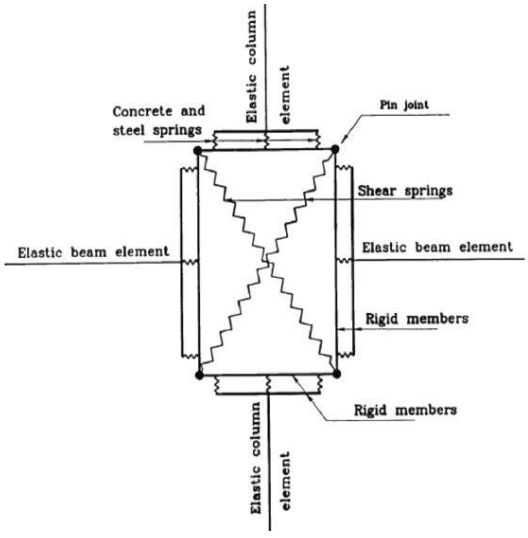

Figure 2-6 Beam-column joint model of Youssef and Ghobarah (2001).

Lowes and Altoontash (2003) developed a joint model consisting of eight bar slip springs and four interface shear springs connecting the beam and column elements to the shear panel zone and one additional spring for the characterization of the shear panel behavior. Figure 2-7 shows the idealization of their proposed model. Similarly, Altoontash and Deierlein (2004) proposed a joint model with inelastic rotational springs connected with multipoint constraints. The behavior of the joint was represented by these four rotational springs located at the beam column ends and at the center of the panel zone as shown in Figure 2-8. The joint model proposed by Shin and LaFave (2004) on the other hand consists of four rigid elements for the panel zone region connected with hinges, three rotational springs located at one of the corners of the joint panel, one rotational spring for the bond slip behavior connected series with another spring for plastic hinge region. Figure 2-9 shows the idealization of this model.

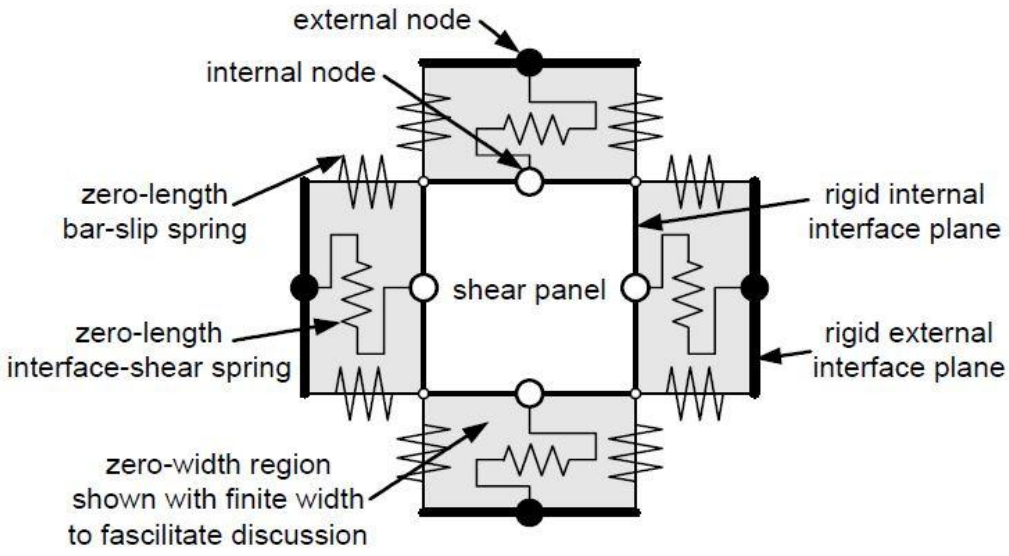

Figure 2-7 Beam-column joint element of Lowes and Altoontash (2003).

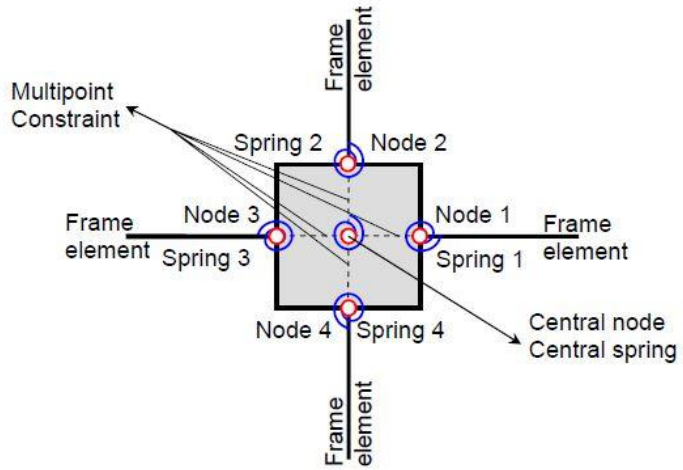

Figure 2-8 Beam-column joint model (Altoontash and Deierlein 2004).

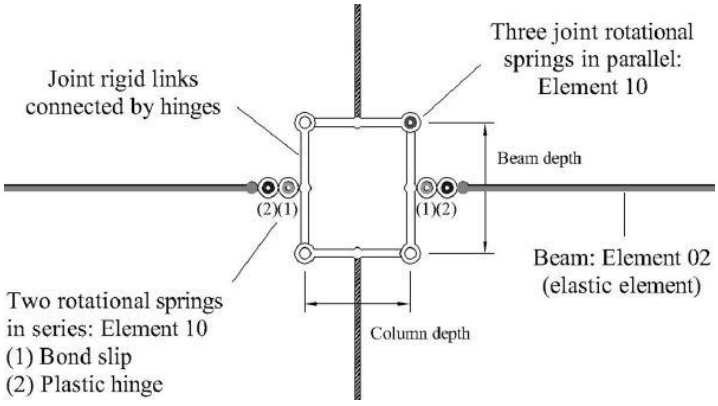

Figure 2-9 Beam-column joint model (Shin and LaFave 2004).

2.3 Previous Studies on Seismic Design Parameters

According to FEMA P695 (FEMA 2009), SPFs include response modification factor (R), system overstrength factor (Ω_0), and deflection amplification factor (C_d). For a better understanding of these parameters, the R factor, which is the primary parameter for seismic design, needs to be explained. Before code regulations and standards on seismic performance factors, R factors were decided based on experiences and observations of known structures (FEMA 2009). It is defined in ATC-19 (ATC 2009) that "the concept of a response modification factor was proposed based on the premise that well-detailed

seismic framing systems could sustain large inelastic deformations without collapse (ductile behavior) and develop lateral strength in excess of their design strength (often termed reserve strength).” It is also explained that “*R* factors were intended to reflect reductions in design force values that were justified on the basis of risk assessment, economics and nonlinear behavior (ATC 1978).”

In 1952, the American Society of Civil Engineers (ASCE) published “Lateral Forces of Earthquake and Wind,” which is today part of ASCE 7-10 (ASCE 2013) , “Minimum Design Loads for Buildings and Other Structures.” Structural Engineers Association of California (SEAOC) appointed a new seismology committee in 1957 to develop a uniform and acceptable building code for structural engineers throughout California. In December, 1959 their work was published as the SEAOC Bluebook (SEAOC 1959). In this book, the equation for base shear *V* was expressed as

$$V = KCW, \tag{2-1}$$

where K is the horizontal force factor, which depends on the building type, *W* is the total dead load, and *C* is a constant, which is a function of the building’s natural period (ATC 19, 1995).

In 1961, Uniform Building Code (IBC 1961), which adopted Bluebook (SEAOC 1959), suggested a *Z* factor which is also called seismic zone factor for different seismic zones, turning Equation (2-2) for design base shear *V* into

$$V=ZKCW. \tag{2-2}$$

The publishing of the “Tentative Provisions for the Development of Seismic Regulations for Buildings ATC-3-06” (ATC 1978) was the turning point for structural engineers with substantial improvements on seismic design regulations when compared to earlier code

regulations. In this report, the *R* factor started to be used in along with the horizontal force factor (*K*), which was the starting point for the response modification factor. The relationship between the *K* factor and the *R* factor was based on judgments and experience of committee members of ATC 3-06 and there was no experimental evidence except for the observations from past earthquakes. It was determined that

$$\mathrm{R} = \frac{5.1}{\mathrm{K}}. \tag{2-3}$$

The next step was the ATC-19 project funded by the National Science Foundation (NSF) and the National Center for Earthquake Engineering Research (NCEER). A report was published in 1995, which includes the new equation for the *R* factor (ATC 1995). The strength, ductility and redundancy were the key parameters for calculating the *R* factor

$$R = R_S . R_\mu . R_R, \tag{2-4}$$

where R_s is the period dependent strength factor, R_μ is the period dependent ductility factor, and R_R is the redundancy factor.

These developments and changes of the *R* factor and its relationship to the *K* factor continued until the publishing of the 2000 edition of the International Building Code (IBC 2000) by International Code Council (ICC), which was a result of the collective study by International Conference of Building Officials (ICBO), Building Officials Code Administrators International (BOCA), and Southern Building Code Congress International (SBCCI). Later on, seismic design guidelines were updated and published in IBC 2000 (2000), IBC 2003 (2003), IBC 2006 (2006) and IBC 2009 (2009). Today ASCE 7-10 is mainly used as a reference for seismic design by structural engineers.

For a structure designed with the current code regulations, the actual strength will be higher than the structure' design strength. This behavior is called the overstrength. The

overstrength is defined as "… a parameter used to quantify the difference between the required and the actual strength of a material" and "overstrength factor" is the ratio between actual strength and required strength (Elnashai and Di Sarno 2008). For a structure, the differences between actual and design material strengths, confinement effect, code conservativeness, oversized members, load combinations, serviceability limit state provisions and contribution of nonstructural elements may cause overstrength (Elnashai and Di Sarno 2008). In addition, neglecting of certain elements such as slab systems and compression braces during design may cause overstrength. Some researchers studied the overstrength factors and their influence on the frame systems during an earthquake. Starting with the study of Freeman et al. (1982), Osteraas and Krawinkler (1990), Uang (1991), Uang and Maarouf (1994), and Elnashai and Mwafy (2002) studied the effect of overstrength factor for structures. In FEMA P695 (FEMA 2009) the equation for overstrength (Ω_o) is expressed as

$$\Omega_o = \frac{V_e}{V}, \tag{2-5}$$

where Ω_o is the overstrength factor, V_e is the maximum strength and V is the design base shear. The overstrength factor is calculated based on the results of a nonlinear static (pushover) analysis, and there is a difference between calculated and code based overstrength factor defined in Table 12.2-1 of ASCE/SEI 7-05 (2006). It is obvious that if the design method changes for a system, the overstrength parameter will also change. Therefore, FEMA P695 the methodology aims to find one overstrength factor that is most appropriate for use in design of a given system (FEMA 2009).

In order to find the total lateral displacement from the elastic displacement, the deflection amplification factor (C_d), which is the third seismic design parameter of the

FEMA P695 (FEMA 2009) methodology needs to be considered. In addition, the deflection amplification factor is used to determine the story drifts for serviceability, to estimate the minimum building separation which may cause pounding, to check the deformation capacity of critical structural members, to account for P-Δ effects, for and detailing of nonstructural members (Uang 1991). ASCE 7-05 (2006) and the NEHRP Provisions (FEMA 2003) define the deflection amplification factors as

$$C_d = \frac{\delta}{\delta e} R. \tag{2-6}$$

In the International Building Code (IBC 2009) and Table 12.2-1 of ASCE/SEI 7-05 (2006), there are guidelines for the selection of deflection amplification factors. The FEMA P695 (FEMA 2009) methodology aims to develop a standard calculation method for the deflection amplification factor for all types of structures.

During the period of the development seismic performance factors, the complexity and number of frame systems have increased. In 2004, FEMA started to a project with ATC to develop a methodology, which is applicable to all type of structures for calculating standardized seismic design parameters. This new methodology developed by the ATC-63 project, known as FEMA P695 (FEMA 2009), was based primarily on the previous methods for seismic design and mostly inspired and covered in the "Tentative Provisions for the Development of Seismic Regulations for Buildings, ATC-3 06" (ATC 1978) and the "Recommended Provisions for Seismic Regulations for New Buildings and Other Structures, 2003" (FEMA 2003). The ATC 63 project members carefully studied previous methods, codes and standards and determined a method for derivation of seismic performance factors (SPFs). They also studied the collapse simulation and nonlinear response of structures evaluated based on incremental dynamic analysis method

(FEMA 2009). The FEMA P695 methodology not only applies directly to new building structures but also conceptually to non-building structures with some limitations (FEMA 2009). Detailed explanation of the FEMA P695 (FEMA 2009) methodology on derivation of seismic design parameters is provided in the following chapter.

Chapter 3 A Review of the FEMA P695 Methodology

3.1 Introduction

The FEMA P695 methodology is a set of calculations to obtain (SPFs) by means of a collapse risk assessment procedure through nonlinear analysis of the systems under consideration. The core of the FEMA P695 methodology is the assessment of the collapse behavior of archetype buildings representing different force resisting systems. To get the collapse behavior of every archetype, nonlinear static and nonlinear dynamic analyses are performed on the models with a set of ground motions scaled up to increasing levels of intensity. The methodology considers both partial and total system collapse. However, it does not account for the local failure of nonstructural members or failure of components that are not a part of the seismic force resisting system. Figure 3-1shows the main elements of the FEMA P695 methodology which are discussed in this chapter. The key elements include collection of test data on materials to define the strength, stiffness and ductility of material and members, collection of design information, calculations of seismic design parameters steps after the nonlinear analyses are completed, and conclusions on the suitability of designs after the evaluation process.

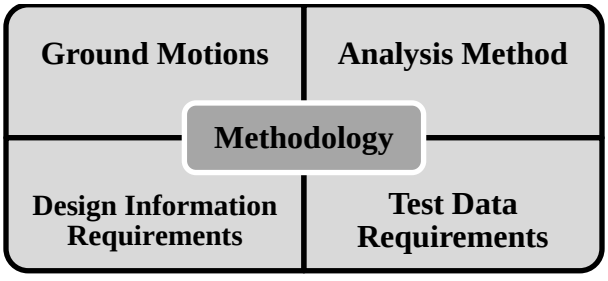

Figure 3-1 Key elements of the FEMA P695 methodology (FEMA 2009).

Well-designed systems and a proper set of maximum considered earthquake (MCE) ground motions are required by the methodology to define the collapse behavior. The

design requirements for the models and the test data for the elements of the structural system are important for the model development. The methodology aims to generalize the analysis methods and the selection of ground motions for most of the structural types for the calculation of SPFs. The methodology uses the NEHRP Provisions (FEMA 2003) and ASCE 7-05 (ASCE 2006) as a guideline for the seismic design of structures and also applies new techniques whenever needed. The methodology sets a low probability for collapse under MCE ground motions to fulfill the life safety objective. It is stated in FEMA P695 (FEMA 2009) that "… rather than attempting to quantify uniform protection of life safety, the Methodology provides approximate uniform protection against the collapse of the structural system" due to difficulties in calculating the risk of loss of life. Safety is defined in terms of collapse margin ratio. Figure 3-2 shows the steps of the derivation process for SPFs.

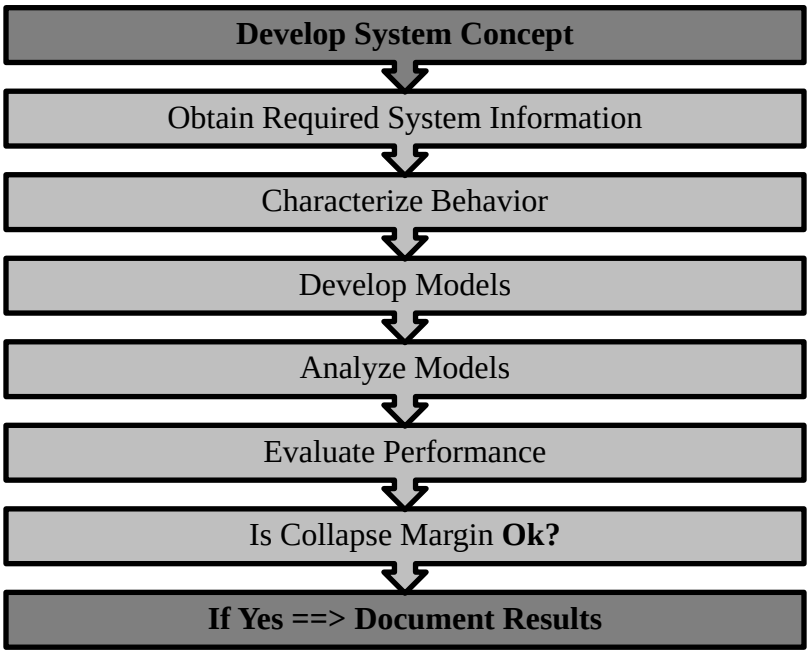

Figure 3-2 Process for quantitatively establishing and documenting SPFs based on FEMA P695 (FEMA 2009)

The steps for the derivation of SPFs:

- Design the archetype seismic force resisting systems for different seismic design categories by changing the bay width, height and the number of stories.
- Collect experimental and analytical data for the development of the analytical models of the archetypes.
- Calculate the overstrength factor and ductility of the system by subjecting every model to nonlinear static pushover analysis.
- Perform nonlinear dynamic analysis for every building model to determine the collapse margin ratio (CMR) and median collapse intensity (S_{MT}). Selected 22 pair of ground motions is scaled up incrementally to define the collapse level of the archetypes. Incremental Dynamic Analysis (IDA) (Vamvatsikos and Cornell 2002) method is used at this step.
- Define the collapse margin ratio (CMR) for each archetype. CMR is the ratio of the median collapse intensity to the maximum considered earthquake (MCE) intensity.
- Calculate the Adjusted Collapse Margin Ratio (ACMR) to account for the spectral shape effects and incorporate the total system collapse uncertainty (β_{TOT}) for comparison against the acceptance criteria.
- If the results meet the minimum design criteria then initial SPFs are assumed correctly. If not, start over with new design parameters and iterate until the minimum criteria are met.

3.2 System Information

The derivation process is based on the nonlinear analysis of the models under predefined earthquake ground motions and evaluation of the collapse behavior of the system. For this reason system information is very important to simulate the correct behavior of the archetypes and obtain reliable seismic design parameters. System information stage includes design requirements based on the codes and standards, limits for the strengths and applications, model configurations, material types and properties, strength and stiffness requirements etc. Experimental test data to validate the properties of the material types and calibration of the nonlinear analysis model are also key points at this stage. After gathering all the information, definition of the acceptable collapse margin ratio concludes the system information stage. The stages for system information are shown in Figure 3-3.

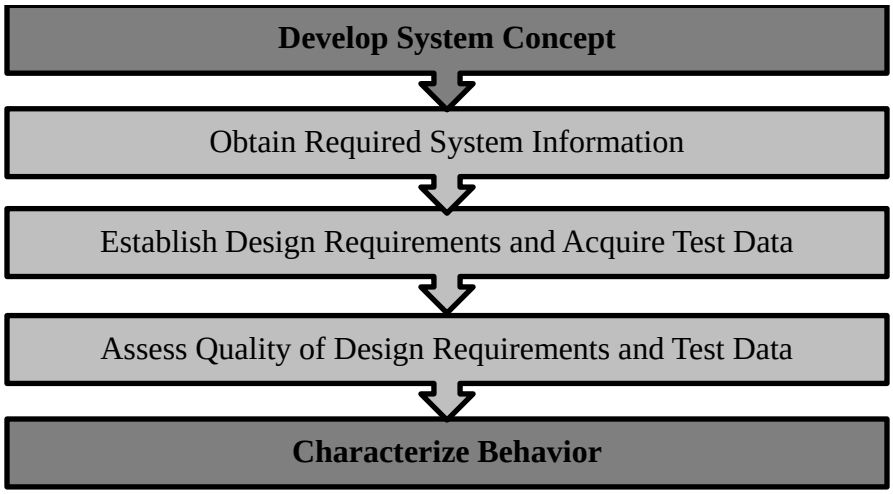

Figure 3-3 Process for obtaining required system information (FEMA 2009)

Once all the system information is gathered, the methodology evaluates the quality of the data and assigns specific quality ratings to the system and experimental test data. Less uncertainty in the design information and experimental data leads to more reliable

seismic design parameters at the end. The quality of the total system collapse uncertainty is related to four parameters: Record-to-Record uncertainty (RTR), Design Requirements Uncertainty (DR), Test Data Uncertainty (TD), and model quality uncertainty (MDL), which are addressed in Section 3.6.3.

3.3 Archetype Development

According to the FEMA P695 methodology, an archetype model is a prototypical representation of a seismic-force-resisting system. These models are intended to represent the behavior of the actual structural system. One of the advantages of archetype models is providing a finite number of trial designs depending on the intended application. In other words, these models are idealizations of the archetype configuration for simulating the behavior of the proposed seismic force resisting systems. The methodology considers them as a connection between the collapse performance evaluation of a single system and the generalized predictions of the behavior for an entire class of buildings (FEMA 2009). Figure 3-4 shows the steps for archetype development.

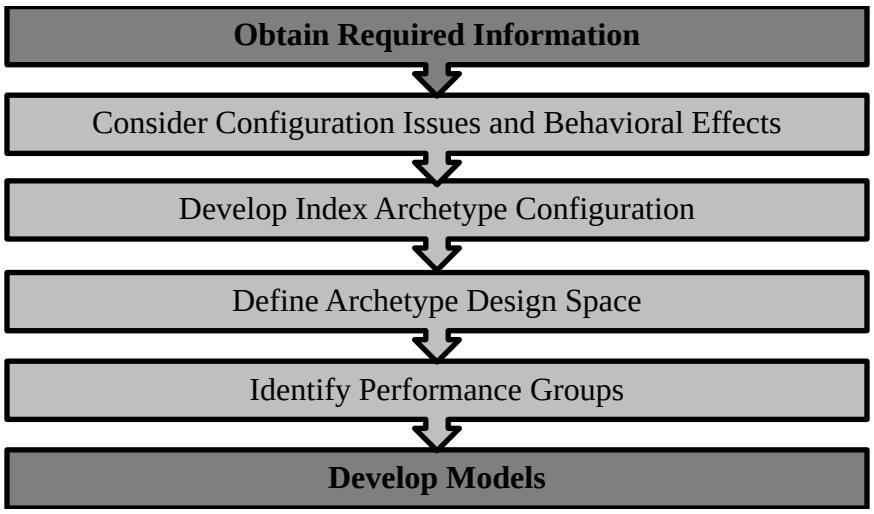

Figure 3-4 Process for development of structural system archetypes (FEMA 2009).

To obtain the collapse performance of structures, the steps need to be clearly defined for archetype development. Index archetype configuration defines the main features and behavior of the seismic force resisting system with a set of building configurations. Detailed information for configuration design variables and related physical properties is given in Table 3-1.

Table 3-1 Configuration design variables and related physical properties (FEMA 2009).

Design Variable	Related Physical Properties
Occupancy and Use	• Typical framing layout • Distribution of seismic-force-resisting system components • Gravity load intensity • Component overstrength
Elevation and Plan Configuration	• Distribution of seismic-force-resisting components • Typical framing layout • Permitted vertical (strength and stiffness) irregularities • Beam spans, number of framing bays, system regularity • Wall length, aspect ratio, plan geometry, wall coupling • Braced bay size, number of braced bays, bracing configuration • Diaphragm proportions, strength, and stiffness (or flexibility) • Ratio of seismic mass to seismic-force-resisting components • Ratio of tributary gravity load to seismic load
Building Height	• Story heights • Number of stories
Structural Component Type	• Moment frame connection types • Bracing component types • Shear wall sheathing and fastener types • Isolator properties and types
Seismic Design Category	• Design ground motion intensity • Special design/detailing requirements • Application limits
Gravity Load	• Gravity load intensity • Typical framing layout • Ratio of tributary gravity load to seismic load • Component overstrength

Archetype design space represents the overall range of accepted configurations, limitations on the seismic force resisting systems and structural design parameters.

Performance groups are for assessment the final behavior of the models in a certain group that shares common features and behavior. The models are evaluated not only individually, but also in groups to obtain their collapse behavior. The groups are formed depending on the structural configurations such as bracing systems, framing spans, story heights and shear wall aspect ratios. Gravity load level is also another factor for the performance groups. While, perimeter and space frames are important for moment frames, bearing walls and non-bearing walls are important for wall systems to distribute the gravity loads (FEMA 2009). Performance groups should also be designed for both maximum and minimum spectral accelerations of a certain seismic design category. As an example, analysis for Seismic Design Category D must cover both SDC D_{max} and SDC D_{min} which refer the maximum and minimum spectral intensities of given category, for assessing the collapse performance of the system. Period domain should also be considered for categorizing the archetype models into performance groups. Variation of fundamental period (T) should be well represented from short period to long period in the index archetype configurations. Index archetype designs reflect the specific structural designs developed for each configuration. The archetype development process concludes with the definition of the fifth and last term called “index archetype models.” These are the computer models for nonlinear analysis of the structures to evaluate the collapse performance under seismic loads.

3.4 Seismic Design Method

The methodology follows the equivalent lateral force (ELF) method defined in ASCE/SEI 7-05 section 12.8 (ASCE 2006) with some exceptions as expressed below.

- If the ELF method is not permitted by ASCE/SEI 7-05 then the response spectrum analysis (RSA) is used.
- If both ELF method and RSA are not permitted by ASCE/SEI 7-05 then RSA method should be used.
- If other methods are commonly used instead of ELF method then RSA method should be used.

Defining SDC is one of the most important steps of the ELF method. The seismic design category is "a classification assigned to a structure based on its occupancy and the severity of the design earthquake ground motion at the site (IBC 2000, ASCE 2006)." While the ASCE/SEI 7-05 defines SDC in terms of five different categories from SDC (A) to SDC (E), the FEMA P695 methodology considers and can be applied to only SDC B, C and D. Because, SDC A structures are not subjected to seismic design and SDC E structures are located MCE ground motion regions. Moreover, the occupancy category which gives information about the end use of structure should be decided before the seismic design. The FEMA P695 methodology assumes that all structures are in occupancy category I and II. For seismic design of the structural system, Design Earthquake (DE) demand is defined in ASCE/SEI 7-05 as two-thirds of MCE demand. Although, the determination of the MCE differs depending on the seismicity region, "the MCE ground motions are uniformly defined as the maximum level of earthquake ground shaking that is considered as reasonable to design normal structures to resist

(Leyendecker et al., 2000).” First, the structures which were designed considering DE as the seismic criteria, then their collapse behavior are assessed according to the MCE seismic design criteria (FEMA 2009). Design procedure starts with the definition of the MCE and then continues with the selection of ground motion response spectral acceleration values for short-period (0.2 second) spectral acceleration, S_S, and 1.0 second spectral acceleration, S_1. Additionally, site coefficients, F_a and F_v are selected. Maximum and minimum spectral acceleration values, design parameters for B, C and D categories, and site coefficient values are given in Table 3-2 and Table 3-3.

Table 3-2 Summary of Mapped Values of Short-Period Spectral Acceleration, S_S, Site Coefficients, F_a, and Design Parameters for Seismic Design Categories B, C, and D, S_{MS} and S_{DS} (FEMA 2009).

Seismic Design Category		Maximum Considered Earthquake			Design
Maximum	Minimum	S_S (g)	F_a	S_{MS} (g)	S_{DS} (g)
D		1.50	1.00	1.50	1.00
C	D	0.55	1.36	0.75	0.50
B	C	0.33	1.53	0.50	0.33
	B	0.156	1.60	0.25	0.167

Table 3-3 Summary of Mapped Values of 1-Second Spectral Acceleration, S_1, Site Coefficients, F_v, and Design Parameters for Seismic Design Categories B, C, and D, S_{M1} and S_{D1} (FEMA 2009).

Seismic Design Category		Maximum Considered Earthquake			Design
Maximum	Minimum	S_1 (g)	F_v	S_{M1} (g)	S_{D1} (g)
D		0.60	1.50	0.90	0.60
C	D	0.132	2.28	0.30	0.20
B	C	0.083	2.40	0.20	0.133
	B	0.042	2.40	0.10	0.067

The transition period (T_s) is defined in the methodology as “the boundary between the region of constant acceleration and the region of constant-velocity of the design (or

MCE) response spectrum" and it is used for the evaluation of short period archetypes (FEMA 2009). The transition period (T_s) is given by

$$T_S = \frac{S_{D1}}{S_{DS}} = \frac{S_{M1}}{S_{MS}}, \quad (3\text{-}1)$$

where the values are given in the above tables.

Determination of the effective seismic weight of structure (W) is the next step of the design procedure. W is calculated based on Section 12.7.2 of ASCE/SEI 7-05 (ASCE 2006), which takes the total dead load of the structure and a minimum of 25% of the reduced floor live load. The methodology uses the ELF method and the design base shear (V) is required for defining the applied forces. The design base shear is

$$V = C_s W, \quad (3\text{-}2)$$

where C_s is the seismic coefficient.

If T$\leq T_s$ then the seismic coefficient is

$$C_S = \frac{S_{DS}}{R}, \quad (3\text{-}3)$$

where R is the trial value of the response modification factor selected for the system design and analysis. If T $> T_s$ then the seismic coefficient is

$$C_S = \frac{S_{DS}}{TR} \geq 0.44 S_{DS}, \quad (3\text{-}4)$$

where T is the fundamental period of the structure calculated based on Section 12.8.2.1 of ASCE 7-05 (ASCE 2006) as

$$T = C_u T_a = C_u C_t h_n^x \geq 0.25\ seconds. \quad (3\text{-}5)$$

The values of the coefficients C_u, C_t, and x are found from Table 12.8-1 and Table 12.8-2 of ASCE/SEI 7-05 (ASCE 2006), and h_n is the height of the building. The importance factor (I) is taken 1.0 for occupancy categories I and II and used in the above

Equations (3-3) and Equation (3-4). Finally, the seismic load combinations are given by the FEMA P695 methodology and Section 12.4 of ASCE 7-05 (ASCE 2006) as follows:

$$(1.2 + 0.2S_{DS})D + Q_E + L, \tag{3-6}$$

$$(0.9 - 0.2S_{DS})D + Q_E, \tag{3-7}$$

$$(1.2 + 0.2S_{DS})D + \Omega_0 Q_E + L, \text{ and} \tag{3-8}$$

$$(0.9 - 0.2S_{DS})D + \Omega_0 Q_E, \tag{3-9}$$

where D and L represent the dead and live load, respectively, and Q_E is for the effect of horizontal seismic-force resulting from the base shear.

3.5 Nonlinear Analysis

The methodology requires both nonlinear static (pushover) and dynamic (response history) analyses of all models to obtain required data for determination of the collapse capacity. The analysis procedure starts with the pushover analysis which also helps with the validation of the model and finishes with the dynamic analysis. The load combination equation of the gravity loads for nonlinear analysis is

$$1.05\text{D} + 0.25\text{L}. \tag{3-10}$$

3.5.1 Nonlinear Static Analysis (Pushover)

One of the main purposes of the pushover analysis is to obtain overstrength (Ω_0) and period based ductility (μ_T) of the archetype building. Once the system reaches a loss of 20% of the maximum base shear then analysis stops (FEMA 2009). The procedure for the pushover analysis is explained in Section 3.3.3 of ASCE/SEI 41-06 (ASCE 2007). The FEMA P695 methodology defines an idealized curve for base shear versus roof displacement as shown in Figure 3-5. V_{max} and V represent the maximum and design base

shear, respectively, the ultimate displacement, (δ_u), and effective roof drift displacement ($\delta_{y,eff}$) are also shown in the Figure 3-5.

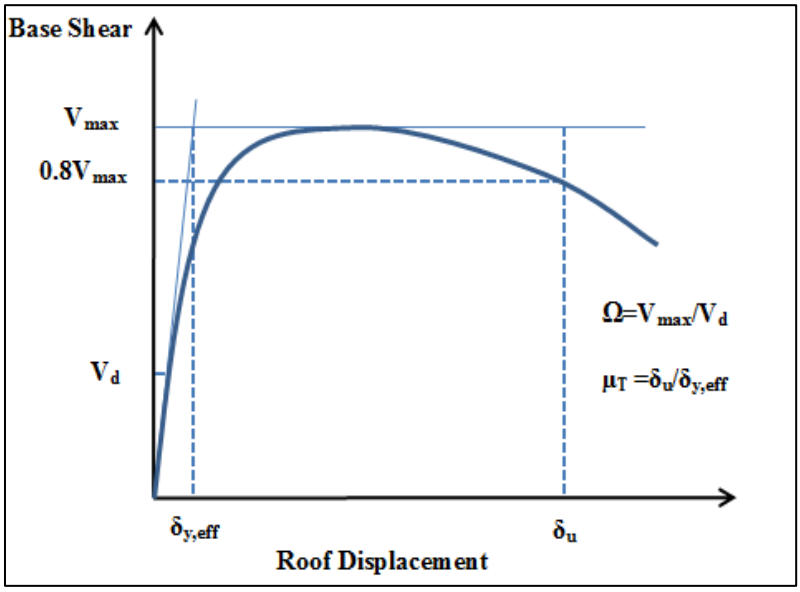

Figure 3-5 Idealized nonlinear static pushover curve.

δ_u is the ultimate roof drift, defined as the point where $0.8V_{max}$ is satisfied and $\delta_{y,eff}$ is the effective yield roof drift displacement ($\delta_{y,eff}$) given by

$$\delta_{y,eff} = C_o \frac{V_{max}}{W} \left[\frac{g}{4\pi^2}\right] (\max(T, T_1))^2, \tag{3-11}$$

where T is fundamental period calculated from equation (3-5), T_1 is the period of the first mode obtained from eigenvalue analysis, g is the gravitational constant gravity, and C_o is the coefficient calculated from Equation C3-4 of ASCE 41-06 (ASCE 2007).

The methodology outlines the information collected from nonlinear static (pushover) and eigenvalue analyses of each index archetype model as

- Fundamental period of vibration, T, model period of vibration, T_1, and design base shear, V
- Distribution of lateral (pushover) loads
- Plot of base shear versus roof drift

- Lateral strength, V_{max}, and static overstrength factor $\Omega_0 = V_{max}/V$
- The effective yield, $\delta_{y,eff}$, and ultimate roof δ_u displacements, and the period based ductility, μ_T
- Story drift ratios at the design base shear, the maximum load V_{max}, and$0.8V_{max}$

3.5.2 Nonlinear Dynamic Analysis (IDA)

Nonlinear dynamic analysis is used to define collapse margin ratios of each archetype. All archetype model responses are evaluated after being subjected to sets of predefined ground motions. The methodology calls the record sets as "Far-Field" and "Near-Field" depending on ground motion record sites distance to fault rapture which is defined as average of Campbell and Joyner-Boore fault distance. The Far-Field record set includes 22 pairs of ground motion records which are recorded greater than or equal to 10 km from the fault rapture. On the other hand, the Near-Field record set includes 28 pairs of ground motion records which are recorded at distances less than 10 km from the fault rapture. In this study Far-Field record set is used for analysis of the models for evaluation of collapse behavior due to the unresolved issues on characterization of near fault hazard and ground motion effects. FEMA P695 provides the record sets that were carefully selected from the Pacific Earthquake Engineering Research Center (PEER) Next-Generation Attenuation (NGA) database (PEER 2006). The record sets meet certain requirements such as consistency with the codes, including a large number of records selections independent of the structural type, very strong ground motions and no special site effects. The list of Far-Field records is given in Table 3-4 and further background information can be found in FEMA P695 (FEMA 2009).

Table 3-4 Summary of Earthquake Event and Recording Station Data for the Far Field Record Set (FEMA 2009).

ID No.	Earthquake			Recording Station	
	M	**Year**	**Name**	**Name**	**Owner**
1	6.7	1994	Northridge	Beverly Hills - Mulhol	USC
2	6.7	1994	Northridge	Canyon Country-WLC	USC
3	7.1	1999	Duzce, Turkey	Bolu	ERD
4	7.1	1999	Hector Mine	Hector	SCSN
5	6.5	1779	Imperial Valley	Delta	UNAMUCSD
6	6.5	1979	Imperial Valley	El Centro Array #11	USGS
7	6.9	1995	Kobe, Japan	Nishi-Akashi	CUE
8	6.9	1995	Kobe, Japan	Shin-Osaka	CUE
9	7.5	1999	Kocaeli, Turkey	Duzce	ERD
10	7.5	1999	Kocaeli, Turkey	Arcelik	KOERI
11	7.3	1992	Landers	Yermo Fire Station	CDMG
12	7.3	1992	Landers	Coolwater	SCE
13	6.9	1989	Loma Prieta	Capitola	CDMG
14	6.9	1989	Loma Prieta	Gilroy Array #3	CDMG
15	7.4	1990	Manjil, Iran	Abbar	BHRC
16	6.5	1987	Superstition Hills	El Centro Imp. Co.	CDMG
17	6.5	1987	Superstition Hills	Poe Road (temp)	USGS
18	7.0	1992	Cape Mendocino	Rio Dell Overpass	CDMG
19	7.6	1999	Chi-Chi, Taiwan	CHY101	CWB
20	7.6	1999	Chi-Chi, Taiwan	TCU045	CWB
21	6.6	1971	San Fernando	LA - Hollywood Sto	CDMG
22	6.5	1976	Friuli, Italy	Tolmezzo	---------

The methodology uses IDA (Vamvatsikos and Cornell 2002) which is a technique to obtain the seismic demand and capacity of the structure after application of scaled ground motions with increasing intensity. IDA uses two limit states to define the collapse behavior: Intensity Measures (IMs) and representative Damage Measures (DMs). The FEMA P695 methodology defines intensity in terms of response spectral acceleration at the fundamental period, T, of the system, except that intensity is defined by the median spectral acceleration of the record set, S_T, rather than by different intensities of individual records (FEMA 2009). DM used in the methodology is the maximum story drift ratio. The results of each analysis are plotted with the median value of collapse spectral acceleration as the ordinate and maximum story drifts as the abscissa. Each IDA curve

shows the result of analysis up to collapse. Once all the analyses of individual records are completed and plotted in a single graph, the median value of the collapse spectral acceleration ($\hat{S}_{CT}$) is calculated as the point for which one half of records cause collapse. Figure 3-6 shows a generic IDA plot, and shows the calculation of collapse margin ratio (CMR).

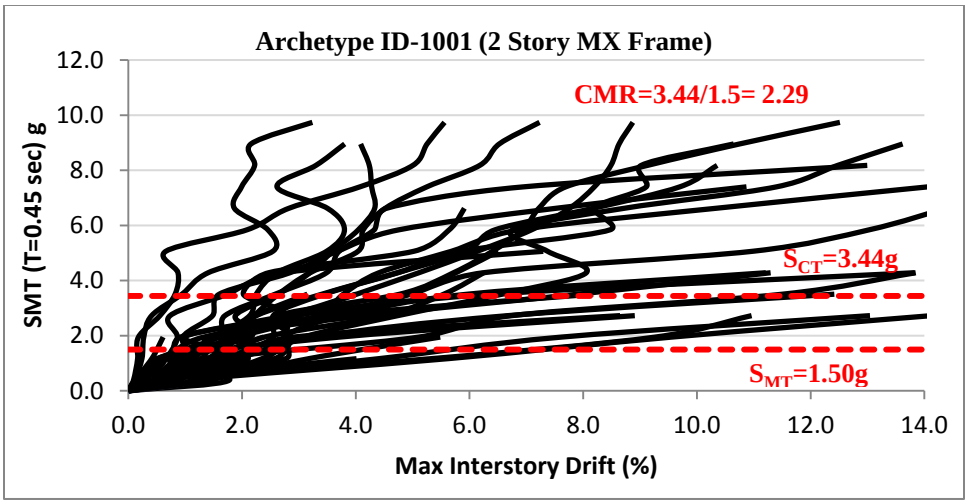

Figure 3-6 Example IDA plot.

As mentioned earlier, the evaluation of the R factor depends on CMR which is defined in FEMA P695 as "the ratio of the ground motion intensity that causes median collapse, to MCE ground motion intensity defined by the building code." By means of nonlinear dynamic analysis of the models explained above, the median collapse capacity ($\hat{S}_{CT}$) is obtained and CMR is calculated as

$$CMR = \frac{\hat{S}_{CT}}{\hat{S}_{MT}}, \tag{3-12}$$

where ($\hat{S}_{CT}$) is the median 5% damped spectral acceleration at the collapse level ground motions and ($\hat{S}_{MT}$) is the 5% damped spectral acceleration of the MCE ground motions.

The MCE ground motion intensity (S_{MT}) for short-period archetypes (i.e. $T \leq T_S$) given by

$$S_{MT} = S_{MS}, \tag{3-13}$$

and for long period archetypes ($T>T_S$) is given by

$$S_{MT} = \frac{S_{M1}}{T}. \tag{3-14}$$

Table 3-5 provides the calculated values for S_{MS}, S_{M1} and T_s for different seismic design categories based on the above equations.

Table 3-5 Summary of Maximum Considered Earthquake Spectral Accelerations And Transition Periods Used for Collapse Evaluation of Seismic Design Category D, C, and B Structure Archetypes (FEMA 2009).

Seismic Design Category		Maximum Considered Earthquake		Transition Period
Maximum	Minimum	***S_{MS} (g)***	***S_{M1} (g)***	***T_s (sec.)***
D		1.50	0.9	0.6
C	D	0.75	0.3	0.4
B	C	0.5	0.2	0.4
	B	0.25	0.1	0.4

The methodology outlines the information reported from nonlinear dynamic analysis of each index archetype model as:

- MCE ground motion intensity (i.e., MCE spectral acceleration), S_{MT}, and the period used to calculate this value,
- Median collapse intensity, $\hat{S}_{CT}$, and collapse margin ratio, *CMR*
- Data used to compute the median collapse capacity, $\hat{S}_{CT}$, along with the response parameter used to identify the collapse condition (e.g., maximum story drift ratio for simulated collapse, and limit-state criteria for non-simulated collapse). Accompanying notes, plots, or narratives describing the governing mode(s) of failure,

- Representative plots of hysteresis curves for selected structural components up to the collapse point.

3.6 Performance Evaluation

Performance evaluation is the final step of the methodology to verify the acceptability of trial values of the response modification factor (R). The results from nonlinear static analysis for the overstrength factor (Ω_0) and results from nonlinear dynamic analysis for the R factor are evaluated and verified against predefined acceptability margins. After the derivation and verification of the R factor, the deflection amplification factor (C_d) is also derived based on the acceptable values of the R factor. The performance evaluation process is explained step by step in Figure 3-7.

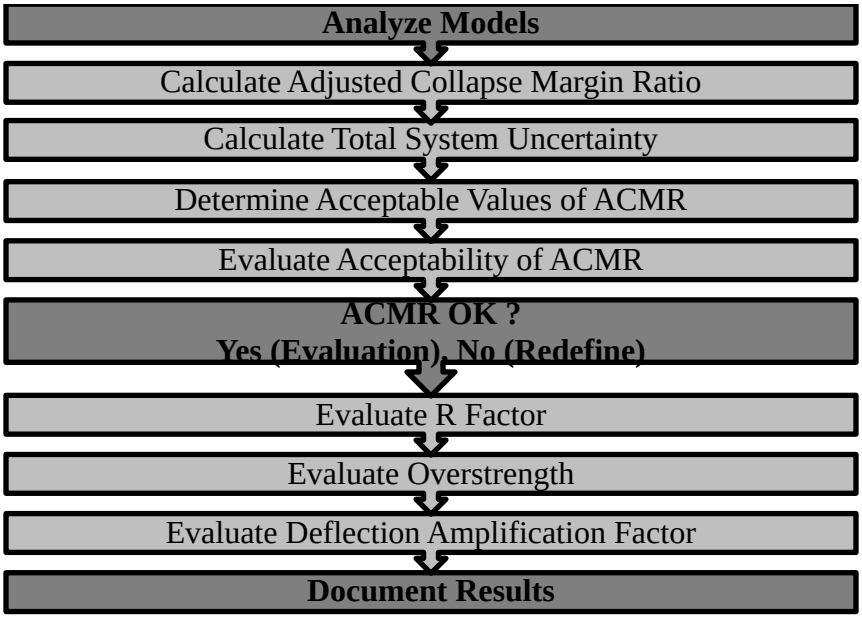

Figure 3-7 Process for performance evaluation (FEMA 2009).

- First step is obtaining the values of overstrength (Ω_0), period-based ductility (μ_T), and collapse margin ratio (CMR) for each archetype from nonlinear analysis.

- Second step is calculating the adjusted collapse margin ratio (ACMR) for each archetype using the spectral shape factor (SSF) which depends on the fundamental period (T) and period-based ductility (μ_T).
- Third step is calculating total system collapse uncertainty (β_{TOT}) based on the quality ratings of design requirements and test data, and the quality rating of index archetype models.
- Fourth step is assessing the adjusted collapse margin ratio (ACMR) for each archetype and average values of ACMR for each archetype performance group relative to acceptable values.
- Fifth step is evaluating the system overstrength factor (Ω_0).
- Last step is evaluating the displacement amplification factor (C_d).

3.6.1 Performance Evaluation Criteria

The definition of performance groups is very important at this stage. The trial values of seismic performance factors (SPFs) are assessed for each performance group. After finding the average value of the performance groups, these values are used for verifying the trials values. The FEMA P695 methodology requires that the trial value of the response modification factor (R) is acceptable for all performance groups. Additionally, the largest average value of the overstrength factor (Ωo) for all performance groups is used. Methodology accepted collapse probability for each performance group's average is limited to 10% and it is limited to 20% for individual archetypes in a group. Once the results are acceptable for the R factor then the deflection amplification factor (C_d) is obtained using a formulation based on the trial R value and system damping factor.

3.6.2 Adjusted Collapse Margin Ratio

CMR is adjusted based on the shape of the spectrum of rare ground motions to account for the spectral shape effect on collapse behavior, structure ductility calculated from nonlinear static analysis, as well as the fundamental period (*T*) of the system. The spectral shape of the ground motion record set, which is carefully selected and grouped for nonlinear dynamic analysis, impacts the collapse capacity as well as CMR. Recent studies show that rare earthquake ground motions have unique spectral shapes, which are different from the mean response spectrum that results in less damaging on structures than expected (Baker and Allin Cornell 2006, Zareian 2006, Haselton and Baker 2006). This effect is accounted for in calculation of adjusted collapse margin ratio with the multiplication of CMR by a simplified spectral shape factor (SSF). The adjusted collapse margin ratio (ACMR) is given by

$$ACMR = SSFxCMR\ . \tag{3-15}$$

Table 3-6 shows the calculated values of the SSF for different SDC Dmax, which is a function of fundamental period (*T*) and ductility (μ) of the system.

Table 3-6 Spectral Shape Factor (SSF) for Archetypes Designed using SDC D_{max} (FEMA 2009).

T (sec.)	Period-Based Ductility, μT							
	1	1.1	1.5	2	3	4	6	≥8
≤ 0,5	1.00	1.05	1.10	1.13	1.18	1.22	1.28	1.33
0.6	1.00	1.05	1.11	1.14	1.20	1.24	1.30	1.36
0.7	1.00	1.06	1.11	1.15	1.21	1.25	1.32	1.38
0.8	1.00	1.06	1.12	1.16	1.22	1.27	1.35	1.41
0.9	1.00	1.06	1.13	1.17	1.24	1.29	1.37	1.44
1.0	1.00	1.07	1.13	1.18	1.25	1.31	1.39	1.46
1.1	1.00	1.07	1.14	1.19	1.27	1.32	1.41	1.49
1.2	1.00	1.07	1.15	1.20	1.28	1.34	1.44	1.52
1.3	1.00	1.08	1.16	1.21	1.29	1.36	1.46	1.55
1.4	1.00	1.08	1.16	1.22	1.31	1.38	1.49	1.58
≥ 1,5	1.00	1.08	1.17	1.23	1.32	1.40	1.51	1.61

3.6.3 Collapse Uncertainty of the System

Uncertainties are very important to obtain correct collapse prediction and they influence the results for CMR. If the system has a well detailed model, enough test data, and reliable design requirements then the same level of life safety can be achieved with a smaller CMR (FEMA 2009). The methodology defines four primary uncertainties as the source of collapse uncertainty and the total uncertainty (β_{TOT}) is calculated by combining all these four uncertainties. Record-to-Record Uncertainty (RTR) arises due to response variation of the archetypes under different seismic records. These variations can be a result of frequency content and dynamic properties of the ground motion records and a result of the hazard peculiarities. Studies show that the record to record uncertainty varies between 0.35 and 0.45 for different structures and earthquake inputs (Haselton and Baker 2006, Ibarra and Krawinkler 2005, Zareian 2006) and the methodology fixed this value (β_{RTR}) to 0.4.

The Design Requirements Uncertainty (DR) is determined based on the quality of the design requirements, and completeness and robustness of these requirements. For the objective of this study, these requirements mostly taken from the ASCE/SEI 7-05, Minimum Design Loads for Buildings and Other Structures (ASCE 2006), and ACI 318, Building Code Requirements for Structural Concrete (ACI 2005) during the system information stage mentioned in Section 3.2. Values for (β_{DR}) are shown in Table 3-7.

The Test Data Uncertainty (TD) is related to the completeness and robustness of the test data used to define the system. The methodology defines the quality of the data for material, component, connection, assembly, and system behavior from experimental investigation and rates them. Values for (β_{TD}) are shown in Table 3-8.

Table 3-7 Quality Rating of Design Requirements (FEMA 2009).

Completeness and Robustness	Confidence in Basis of Design Requirements		
	High	Medium	Low
High. Extensive safeguards against unanticipated failure modes. All important design and quality assurance issues are addressed.	(A) Superior β_{DR} = 0.10	(B) Good β_{DR} = 0.20	(C) Fair β_{DR} = 0.35
Medium. Reasonable safeguards against unanticipated failure modes. Most of the important design and quality assurance issues are addressed.	(B) Good β_{DR} = 0.20	(C) Fair β_{DR} = 0.35	(D) Poor β_{DR} = 0.50
Low. Questionable safeguards against unanticipated failure modes. Many important design and quality assurance issues are not addressed.	(C) Fair β_{DR} = 0.35	(D) Poor β_{DR} = 0.50	--

Table 3-8 Quality Rating of Test Data from an Experimental Investigation Program (FEMA 2009).

Completeness and Robustness	Confidence in Test Results		
	High	Medium	Low
High. Material, component, connection, assembly, and system behavior well understood and accounted for. All, or nearly all, important testing issues addressed.	(A) Superior β_{TD} =0.10	(B) Good β_{TD} =0.20	(C) Fair β_{TD} =0.35
Medium. Material, component, connection, assembly, and system behavior generally understood and accounted for. Most important testing issues addressed.	(B) Good β_{TD} = 0.20	(C) Fair β_{TD} =0.35	(D) Poor β_{TD} =0.50
Low. Material, component, connection, assembly, and system behavior fairly understood and accounted for. Several important testing	(C) Fair β_{TD} = 0.35	(D) Poor β_{TD} =0.50	--

The fourth and the last major uncertainty used in the calculation of the total uncertainty of the system is Modeling Uncertainty (MDL). It is rated based on the quality

of the index archetype models and simulation capabilities of these models for capturing collapse behavior. Values for (β_{MDL}) are shown in Table 3-9.

Table 3-9 Quality Rating of Index Archetype Models (FEMA 2009).

Representation of Collapse Characteristics	Accuracy and Robustness of Models		
	High	**Medium**	**Low**
High. Index models capture the full range of the archetype design space and structural behavioral effects that contribute to collapse.	(A) Superior β_{MDL}= 0.10	(B) Good β_{MDL} = 0.20	(C) Fair β_{MDL} = 0.35
Medium. Index models are generally comprehensive and representative of the design space and behavioral effects that contribute to collapse.	(B) Good β_{MDL} = 0.20	(C) Fair β_{MDL} = 0.35	(D) Poor β_{MDL} = 0.50
Low. Significant aspects of the design space and/or collapse behavior are not captured in the index models.	(C) Fair β_{MDL} = 0.35	(D) Poor β_{MDL} = 0.50	--

Once the uncertainties and their values are found, the total system collapse uncertainty (β_{TOT}) is obtained as

$$\beta_{TOT} = \sqrt{\beta_{RTR}{}^2 + \beta_{DR}{}^2 + \beta_{TD}{}^2 + \beta_{MDL}{}^2}\,. \tag{3-16}$$

Based on these uncertainties βTOT values are given in the Table 3-10

Table 3-10 Total System Collapse Uncertainty Values (FEMA 2009).

Model Quality ((A) Superior)				
Quality of Test Data	Quality of Design Requirements			
	(A) Superior	(B) Good	(C) Fair	(D) Poor
(A) Superior	0.425	0.475	0.550	0.650
(B) Good	0.475	0.500	0.575	0.675
(C) Fair	0.550	0.575	0.650	0.725
(D) Poor	0.650	0.675	0.725	0.825
Model Quality ((B) Good)				
Quality of Test Data	Quality of Design Requirements			
	(A) Superior	(B) Good	(C) Fair	(D) Poor
(A) Superior	0.475	0.500	0.575	0.675
(B) Good	0.500	0.525	0.600	0.700
(C) Fair	0.575	0.600	0.675	0.750
(D) Poor	0.675	0.700	0.750	0.825
Model Quality ((C) Fair)				
Quality of Test Data	Quality of Design Requirements			
	(A) Superior	(B) Good	(C) Fair	(D) Poor
(A) Superior	0.550	0.575	0.650	0.725
(B) Good	0.575	0.600	0.675	0.750
(C) Fair	0.650	0.675	0.725	0.800
(D) Poor	0.725	0.750	0.800	0.875
Model Quality ((D) Poor)				
Quality of Test Data	Quality of Design Requirements			
	(A) Superior	(B) Good	(C) Fair	(D) Poor
(A) Superior	0.650	0.675	0.725	0.825
(B) Good	0.675	0.700	0.750	0.825
(C) Fair	0.725	0.750	0.800	0.875
(D) Poor	0.825	0.825	0.875	0.950

3.6.4 Evaluation of the Seismic Parameters

After finding ACMR, it is compared with the acceptable collapse margin values which are predetermined with consideration of the total uncertainty (β_{TOT}) and collapse probability limits. Acceptable values of ACMR are given by FEMA P695 based on the total uncertainty and acceptable collapse probability as shown in Table 3-11.

Table 3-11 Acceptable Values of ACMR (ACMR10% and ACMR 20%) (FEMA 2009).

Total System Collapse Uncertainty	Collapse Probability				
	5%	10% ACMR 10%)	15%	20% ACMR 20%)	25%
0.275	1.57	**1.42**	1.33	**1.26**	1.20
0.300	1.64	**1.47**	1.36	**1.29**	1.22
0.325	1.71	**1.52**	1.40	**1.31**	1.25
0.350	1.78	**1.57**	1.44	**1.34**	1.27
0.375	1.85	**1.62**	1.48	**1.37**	1.29
0.400	1.93	**1.67**	1.51	**1.40**	1.31
0.425	2.01	**1.72**	1.55	**1.43**	1.33
0.450	2.10	**1.78**	1.59	**1.46**	1.35
0.475	2.18	**1.84**	1.64	**1.49**	1.38
0.500	2.28	**1.90**	1.68	**1.52**	1.40
0.525	2.37	**1.96**	1.72	**1.56**	1.42
0.550	2.47	**2.02**	1.77	**1.59**	1.45
0.575	2.57	**2.09**	1.81	**1.62**	1.47
0.600	2.68	**2.16**	1.86	**1.66**	1.50
0.625	2.80	**2.23**	1.91	**1.69**	1.52
0.650	2.91	**2.30**	1.96	**1.73**	1.55
0.675	3.04	**2.38**	2.01	**1.76**	1.58
0.700	3.16	**2.45**	2.07	**1.80**	1.60
0.725	3.30	**2.53**	2.12	**1.84**	1.63
0.750	3.43	**2.61**	2.18	**1.88**	1.66
0.775	3.58	**2.70**	2.23	**1.92**	1.69
0.800	3.73	**2.79**	2.29	**1.96**	1.72
0.825	3.88	**2.88**	2.35	**2.00**	1.74
0.850	4.05	**2.97**	2.41	**2.04**	1.77
0.875	4.22	**3.07**	2.48	**2.09**	1.80
0.900	4.39	**3.17**	2.54	**2.13**	1.83
0.925	4.58	**3.27**	2.61	**2.18**	1.87
0.950	4.77	**3.38**	2.68	**2.22**	1.90

3.6.4.1 Response Modification Factor Evaluation (*R*)

R factor should not only be evaluated individually but also be evaluated as a group, and meet two criteria:

- The probability of collapse for MCE ground motions is 10%, or less, on average for all index archetype designs, i.e.,

$$\overline{ACMRi} \geq ACMR_{10\%}. \quad (3\text{-}17)$$

- The probability of collapse for MCE ground motions is approximately 20%, or less, for each index archetype, i.e.,

$$ACMR_1 \geq ACMR_{20\%}. \quad (3\text{-}18)$$

Finally, ACMR is higher than the acceptable values for individual and each performance group then the trial values of the R factor are acceptable. If not, redesign process is required starting with a new trial value for the R factor.

3.6.4.2 Evaluation of the Overstrength Factor (Ωo)

Nonlinear static analysis is used to calculate the archetype overstrength (Ω) for all performance groups. The average value is then calculated for each group. The system overstrength factor (Ω_0) used for the design cannot be taken less than that value. It should be rounded to the half unit intervals and it should not be taken larger than 1.5 times the R factor. Due to the code restrictions, 3.0 is its practical limit defined in Table 12.2-1 of ASCE/SEI 7-05 (2006) for all current approved seismic force resisting systems.

3.6.4.3 Evaluation of the Deflection Amplification Factor (C_d)

The deflection amplification factor (C_d) is derived based on the acceptable values of the R and damping factors. The equation given by the methodology is

$$C_d = \frac{R}{B_I}, \quad (3\text{-}19)$$

where BI is a numerical coefficient for damping that depends on the effective damping (β I) and period of the system. The value for BI for a critical damping value of 5% is 1.0 according to Table 18.6-1 of ASCE 7-05 (2006), which means that for most of the systems deflection amplification factor (*Cd*) is equal to the R factor. This equality also can be explained by the "Newmark rule" which assumes that the inelastic displacement is approximately equal to the elastic displacement at the roof for structures with long

periods. Here the damping coefficients for the MX and R/ECC frames are calculated by means of reverse cyclic pushover analysis and the detailed computation and results are provided in Chapter 6.

Chapter 4 Archetype Development Procedure

4.1 Material Properties

It is well know that the response of a structure under earthquake loading mostly depends on the quality and type of construction materials. Due to different demands of the structures, the designers and researchers have been trying to find the most suitable construction material, as well as the most suitable properties for a better performance for a particular project. Here, during the archetype development procedure two types of materials: conventional steel reinforced concrete and steel reinforced ECC are used. The material properties of interest were outlined by the FEMA P695 methodology as follows:

1. Tensile, compressive, and shear stress and strain properties,
2. Friction properties between parts,
3. Young's modulus,
4. Bond properties at the interface of the two materials, and
5. Other properties on which component behavior depends on strongly.

The relevant properties for modeling in this study are items 1 and 3. These parameters are chosen from the existing codes and standards, and prior experimental programs. Additionally, considering the study of Mander et al. (1988), the confinement effect, which has a major influence on both strength and ductility of concrete, is taken into consideration for conventional concrete members. The calculated values for the members of the frames considered here vary between 1.03 and 1.25 depending on the material and section properties.

4.1.1 Conventional Concrete

As mentioned earlier, the estimation of overall structural response under the static and dynamic loading depends on the correct prediction of the material behavior. For RC and MX frames, the properties of concrete are directly taken from a detailed study on 30 code-conforming reinforced concrete special moment frame buildings (Haselton and Deierlein 2008). Figure 4-1 shows the uniaxial constant confinement concrete model developed by Martinez-Rueda and Elnashai (1997) based on the study of Mander et al. (1988). The four key parameters of the model are the compressive strength of unconfined concrete (f'c), the tensile strength of concrete (ft), the crushing strain (Ɛco), and the confinement factor (K). Table 4-1 gives the parameters of the concrete material model.

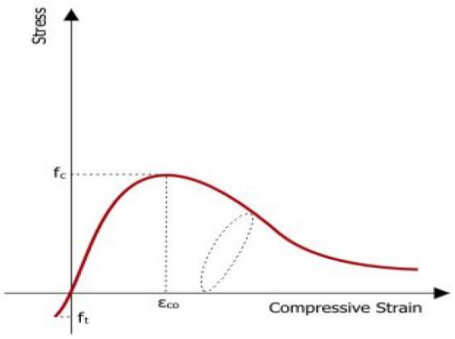

Figure 4-1 The uniaxial constant confinement concrete model (Martínez-Rueda and Elnashai 1997).

Table 4-1 The properties of concrete for the "con2" material model

Property	Description	Value
f_c	Compressive strength	34.47 to 48.26 N/mm^2
f_t	Tensile strength	0.1*f_c
$\mathcal{E}_{co}$	Crushing strain	0.002
K	Confinement factor	1.03 to 1.25

Here, the confinement factor (K) is calculated using the equations in Mander et al. (1988).

4.1.2 Engineered Cementitious Composites

Engineered Cementitious Composites (ECC) is a class of high performance fiber reinforced composite material (HPFRCC) designed based on micromechanical principals. The main advantages of ECC over conventional concrete are providing high ductility strength in tension, multiple cracks with reduced crack widths instead of concentrated large cracks, and high energy dissipation capacity (Li and Wu 1992, Li 1992a, Li and Leung 1992, Gencturk and Elnashai 2011). In addition, it was observed that the high deformability of ECC in tension results in enhanced bond characteristics between reinforcing bars and the surrounding matrix, thereby, improving several behavioral features of reinforced ECC members including stiffness and strength (Fischer and Li 2002). By means of a well-defined ECC constitutive model, the behavior of the structure can be captured under various load conditions. For R/ECC and MX frames; the constitutive model developed by Gencturk and Elnashai (2013) is used to model ECC material. Figure 4-2 shows the envelope curves for the ECC model in compression and tension. The parameters required for modeling are shown in

Table 4-2 including the values used in this study.

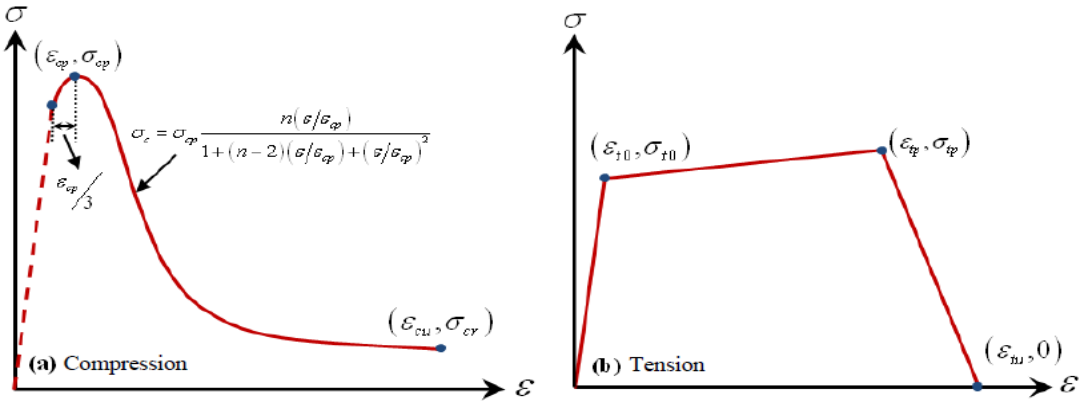

Figure 4-2 The material model for "ecc" [Elnashai et al. (2010)].

Table 4-2 Material properties of "ecc" model.

Property	Description	Value
E	The Young's modulus	25000
ε_{t0}	First cracking strain	1.0E-4
ε_{tp}	Strain at peak stress in tension	0.025
σ_{tp}	Strength in tension	3.6
ε_{tu}	Tensile strain capacity	0.035
ε_{cp}	Strain at peak stress in compression ($\varepsilon_{cp} < 0$)	-0.003
σ_{cp}	Strength in compression ($\sigma_{cp} < 0$)	-55
ε_{cu}	Ultimate strain in compression ($\varepsilon_{cu} < 0$).This value should always be less than the maximum compressive strain expected during analysis	-0.3
σ_{cr}	Stress on the compression envelope corresponding to ε_{cu} ($\sigma_{cr} < 0$)	-4.65

4.2 Steel

Grade 60 steel which is consistent with the American Society for Testing and Materials (ASTM) A 615 standards is used as the longitudinal and transverse reinforcement. A constitutive model based on the Ramberg-Osgood model with kinematic strain-hardening (Ramberg and Osgood 1943) is used for the modeling of the steel behavior. Figure 4-3 shows a sample stress strain response of this model and Table 4-3 provides the definition of each parameter and the values used.

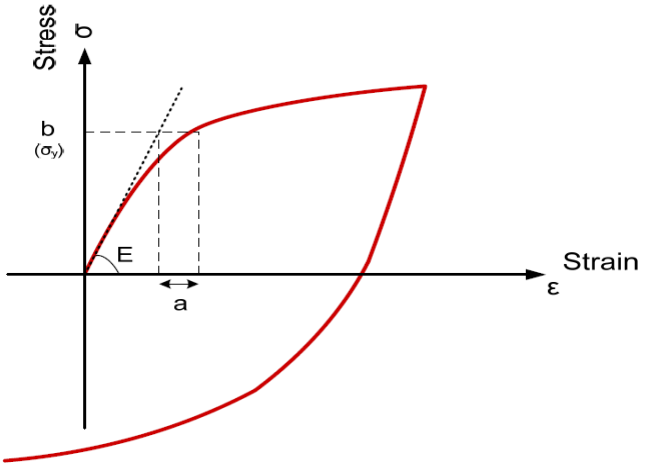

Figure 4-3 The Ramberg-Osgood steel material model.

Table 4-3 Material Properties of the Steel Model.

Property	Description	Value
E	The Young's modulus	200000
a	Material constants determined by a best-fit procedure using the available experimental data.	0.005
b	Material constants determined by a best-fit procedure using the available experimental data.	380
n	Material constants determined by a best-fit procedure using the available experimental data.	11

4.3 Loads

The gravity loads for nonlinear analysis are calculated using Equation (3-10). The design floor dead and live loads are taken as 8379 N/m2 (175 psf) and 2394 N/m2 (50 psf), respectively, for all the structural types.

4.4 Frame Types and Configurations

In parallel with the objectives of this study, three types of special moment frames (SMF): a reinforced concrete frames (RC), a reinforced ECC frame (R/ECC), and a concrete and ECC, multi material mixed frames (MX), are modeled to derive the seismic design parameters. RC frame serves as a control group. Based on the FEMA P695 findings; buildings designed in low seismic regions (D_{min}) have a lower collapse risks than buildings designed in high seismic regions (D_{max}). Moreover, increasing bay width results in a reduced collapse risk. For instance, a 9144 mm (30-foot) bay width building has a higher CMR compared to a 6096 mm (20-foot) bay width building. Therefore, in order to derive the seismic design parameters, buildings with two different bay widths: 6096 mm (20-ft) and 9144 mm (30-foot), in high seismic design category, are chosen here with variable story heights (Haselton and Deierlein 2008). Each frame type has the same number of models covering a wide range of buildings from 1-story to 20-story. As

the story height, 4572 mm (15-ft) is used for the first story while 3962 mm (13-ft) is used for the remainder. The details about the performance groups, which were divided into subgroups with respect to bay width, story numbers and seismic framing systems, are given in Section 4.5.

4.4.1 Reinforced Concrete Frames (R/C)

Based on the performance evaluation of the FEMA P695 methodology, 12 different SMF archetype models are chosen from the study of Haselton and Dierlein (2008). The same models are used for RC, MX and R/ECC frames. The Table 4-4 gives the properties of the frames, and the detailed design documentation is given in Appendix A.

4.4.2 Reinforced ECC Frames (R/ECC)

The deformability of the structures depends on the behavior of the structural members. Replacement of the conventional concrete with ECC increases the inelastic deformation capacity without any loss of load carrying capacity. R/ECC is modeled using the same dimensions and reinforcement configuration with RC frames. It is acknowledged that the use of ECC results in a higher cost than the conventional concrete (Gencturk and Elnashai 2011); however the cost analysis is beyond the scope of this study.

4.4.3 Multi Material Frames (MX)

The beam column joint regions are one of the most critical parts of building structures due to complex load transfer mechanisms and nonlinear behavior of materials during earthquakes. In order to improve the seismic performance, beam-column joint panel zones and plastic hinge regions of RC frames are modeled using ECC in MX frames. Although it is relatively easy to define the dimension of the beam column joint region,

there are numerous expressions for calculating the plastic hinge lengths. The plastic hinge region is defined as "length of frame element over which flexural yielding is intended to occur due to design displacements, extending not less than a distance *h* from the critical section where flexural yielding initiates" (ACI 2008). For simplicity, the plastic hinge length is assumed equal to the depth of the beam and column elements (h_1, h_2) as shown in Figure 4-4 (Blume, Newmark, and Corning 1961).

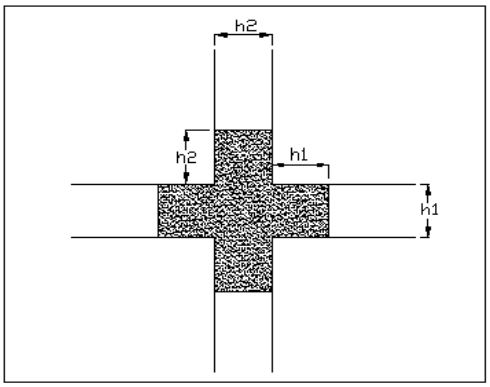

Figure 4-4 Illustration of beam-column plastic hinge length.

Table 4-4 Properties of RC SMF Archetype Buildings.

Archetype ID (R/C)	Archetype ID (R/ECC)	Archetype ID (MX)	Num. of Stories	Frame Type	SDC	Bay Width
2061-RC	2061-RECC	2061-MX	1	S	D_{max}	6096 mm
2069-RC	2069-RECC	2069-MX	1	P	D_{max}	6096 mm
2064-RC	2064-RECC	2064-MX	2	P	D_{max}	6096 mm
1001-RC	1001-RECC	1001-MX	2	S	D_{max}	6096 mm
1003-RC	1003-RECC	1003-MX	4	P	D_{max}	6096 mm
1008-RC	1008-RECC	1008-MX	4	S	D_{max}	6096 mm
1011-RC	1011-RECC	1011-MX	8	P	D_{max}	6096 mm
1012-RC	1012-RECC	1012-MX	8	S	D_{max}	6096 mm
1013-RC	1013-RECC	1013-MX	12	P	D_{max}	6096 mm
1014-RC	1014-RECC	1014-MX	12	S	D_{max}	6096 mm
1020-RC	1020-RECC	1020-MX	20	P	D_{max}	6096 mm
1021-RC	1021-RECC	1021-MX	20	S	D_{max}	6096 mm
1009-RC	1009-RECC	1009-MX	4	P	D_{max}	9144 mm
1010-RC	1010-RECC	1010-MX	4	S	D_{max}	9144 mm

4.5 Performance Groups

The seismic design parameters are derived for each performance group and the performance groups are determined depending on the building configuration, gravity load level, seismic design category, and period domain. Each group has to contain at least three archetypes, and every system has to include at least four performance groups (FEMA 2009). Following to FEMA P695 methodology, two extra three-story archetypes are added to PG-1 and PG-5 for proper application of the methodology. Results for these newly defined archetypes calculated from the average values of two-story and four-story archetypes. FEMA P695 provides the performance group summary according to Table 4-5 by considering these key parameters mentioned above.

Table 4-5 Performance Groups for Evaluating RC SMFs

Performance Group Summary					
Group No	Grouping Criteria				Number of Archetypes
	Basic Config.	Design Load Level		Period Domain	
		Gravity	Seismic		
PG-1	6096 mm Bay Width	High (Space Frame)	SDC D_{max}	Short	2+1
PG-2				Long	4
PG-3			SDC D_{min}	Short	0
PG-4				Long	0
PG-5		Low (Perimeter Frame)	SDC D_{max}	Short	2+1
PG-6				Long	4
PG-7			SDC D_{min}	Short	0
PG-8				Long	0
PG-10	9144 mm Bay Width	Low (Perimeter Frame)	SDC D_{max}	Long	1
PG-14		High (Space Frame)	SDC D_{max}	Long	1

Chapter 5 Nonlinear Analysis of Archetypes

5.1 Nonlinear Analysis Program (ZEUS NL)

Accurate modeling of the buildings is of utmost importance for collapse simulation, which is directly related to the derivation of seismic design parameters. Beams, columns and beam-column joint regions need to be represented properly by the modeling approach. Due to its accuracy and efficiency, fiber-based element modeling approach is used here for the model development. ZEUS NL finite element software (Elnashai, Papanikolaou, and Lee 2010), which was developed at the Mid-America Earthquake Center (MAE Center) for inelastic analysis and simulation of structures under both dynamic and static loading conditions, is used here. The program uses the fiber approach to define the structural behavior; it accounts for large inelastic displacements, and has a robust numerical solver. Wide range of analysis types can be performed by ZEUS NL such as eigenvalue, static pushover, static time-history, and dynamic analysis. The following material models are available in ZEUS NL:

- **stl0:** Linear elastic model
- **stl1:** Bilinear elasto-plastic model with kinematic strain-hardening
- **stl2:** Ramberg-Osgood model with masing type hysteresis curve
- **stl3:** Menegotto-Pinto model with isotropic strain-hardening
- **con1:** Trilinear concrete model
- **con2:** Uniaxial constant confinement concrete model
- **con3:** Uniaxial variable confinement concrete model
- **con4:** Sheikh-Uzumeri model
- **ecc:** Model for ECC materials

- **frp1:** Uniaxial constant fiber-reinforced plastic confined concrete model.

Besides accuracy and computational efficiency of ZEUS NL, existence of the "ECC" material model (Gencturk and Elnashai 2011) is another advantage for the development and analysis of high performance material buildings in this thesis. Due to these advantages, ZEUS NL software package is used in this study for structural simulation of the developed archetype buildings.

5.2 Input Ground Motions

As reviewed in Section 3.5.2, the methodology defines record sets as "Far-Field" and "Near-Field" depending on their location to fault rapture. The Far-Field record set includes 22 pairs of ground motion records, which are recorded at distances larger than or equal to 10 km from the fault rapture. On the other hand, the Near-Field record set includes 28 pairs of ground motions records, which are recorded at the distances under 10 km from the fault rapture. In this study Far-Field record set is used for analysis of the models for collapse evaluation and this record set is applicable to all SDCs and soil site classifications. The list of Far Field record set is given in Table 3-4.

5.2.1. Normalization of Records

Although Far-Field records are selected carefully with consideration of magnitude, source type, site conditions and some other related parameters; they still need to be normalized to reduce variability between the records. Normalization of the records is done based on their peak ground velocity (PGV) values. The geometric mean of PGV of the two horizontal components is obtained first. Formulation defined by the methodology is given below with Equation (5-1 as

$$\mathrm{NM} = \frac{Median(PGV_{PEER})}{PGV_{PEER}}, \tag{5-1}$$

where NM = Normalization factor for both horizontal components of the record,

PGV_{PEER} = Peak ground velocity of the record (PEER NGA database),

Median (PGV_{PEER}) = Median of PGV_{PEER} of the record set.

PGV and calculated values of the normalization factor are given in Table 5-1.

Table 5-1 Factors Used to Normalize Recorded Ground Motions and Parameters of Normalized Ground Motions for the Far-Field Record Set (FEMA 2009).

ID NO	Recorded Parameters			Normalization Factor	Normalized Motions	
	1-sec Spec. Acc. (g)		PGV_{PEER} (cm/s.)		PGA max (g)	PGV max (g)
	Comp.1	Comp. 2				
1	1.02	0.94	57.2	0.65	0.34	41
2	0.38	0.63	44.8	0.83	0.40	38
3	0.72	1.16	59.2	0.63	0.52	39
4	0.35	0.37	34.1	1.09	0.37	46
5	0.26	0.48	28.4	1.31	0.46	43
6	0.24	0.23	36.7	1.01	0.39	43
7	0.31	0.29	36.0	1.03	0.53	39
8	0.33	0.23	33.9	1.10	0.26	42
9	0.43	0.61	54.1	0.69	0.25	41
10	0.11	0.11	27.4	1.36	0.30	54
11	0.50	0.33	37.7	0.99	0.24	51
12	0.20	0.36	32.4	1.15	0.48	49
13	0.46	0.28	34.2	1.09	0.58	38
14	0.27	0.38	42.3	0.88	0.49	39
15	0.35	0.54	47.3	0.79	0.40	43
16	0.31	0.25	42.8	0.87	0.31	40
17	0.33	0.34	31.7	1.17	0.53	42
18	0.54	0.39	45.4	0.82	0.45	36
19	0.49	0.95	90.7	0.41	0.18	47
20	0.30	0.43	38.8	0.96	0.49	38
21	0.25	0.15	17.8	2.10	0.44	40
22	0.25	0.30	25.9	1.44	0.50	44
Median (PGVPEER)			37.2			

5.2.2. Scaling of Records

Second step is scaling of the record set to a level such that half of the records cause collapse of the models. This scaling is done to determine the median collapse capacity,

S_{CT}, which is used for calculating CMR. The FEMA P695 methodology states that "In high seismic regions where buildings are at greatest risk, few recorded ground motions are intense enough, and significant upward scaling of the records is often required" (FEMA 2009). Both normalization and scaling steps meet the ground motion scaling requirements of Section 16.1.3.2 of ASCE/SEI 7-05 (2006).

5.3 Eigenvalue Analysis

Fundamental period (T_1) of the archetype models are determined by an eigenvalue analysis. T_1 values are used in Equation (3-11) for calculating $\delta_{y,eff}$, which is the main input for the computation of the period based ductility. Calculated values of fundamental periods are given in Table 5-2. Eigenvalue analysis results show that R/ECC frames have the highest T_1 values and RC frames have the lowest for all archetype models.

5.4 Nonlinear Static (Pushover) Analysis

The main purpose of the pushover analysis is to obtain (Ω_0) for the archetype buildings, which is defined as the ratio of (V_{max}) to (V_d) and to obtain (μ_T), which is the ratio of ultimate roof displacement (δ_u) to effective yield displacement ($\delta_{y,eff}$). Once the system reaches to a loss of 20% of the maximum base shear then analysis meets the requirements (FEMA 2009). The procedure for the pushover analysis is explained in Section 3.3.3 of ASCE/SEI 41-06 (2007). As described in Section 3.5.1; the base shear values (V), effective and ultimate roof drift values, story drift values are obtained from the static pushover analysis. Figure 5-1, Figure 5-2, Figure 5-3 and Figure 5-4 show the example pushover analysis result for model ID-2064 RC, MX and R/ECC frames.

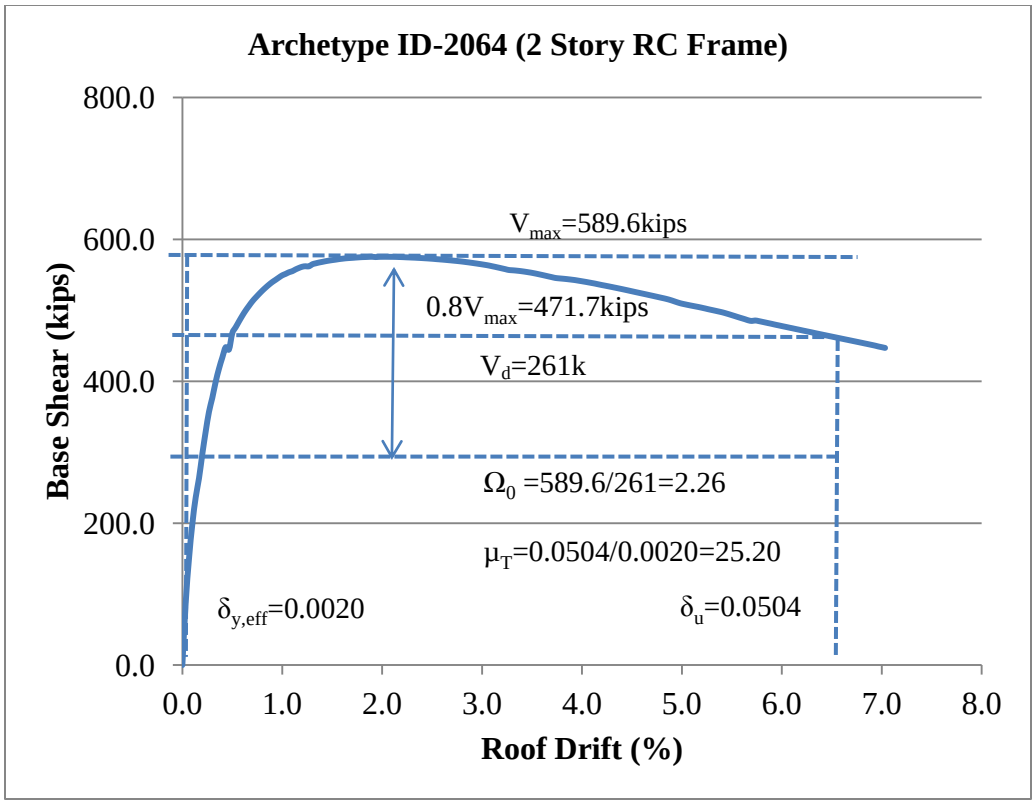

Figure 5-1 Pushover analysis result for model ID-2064 RC.

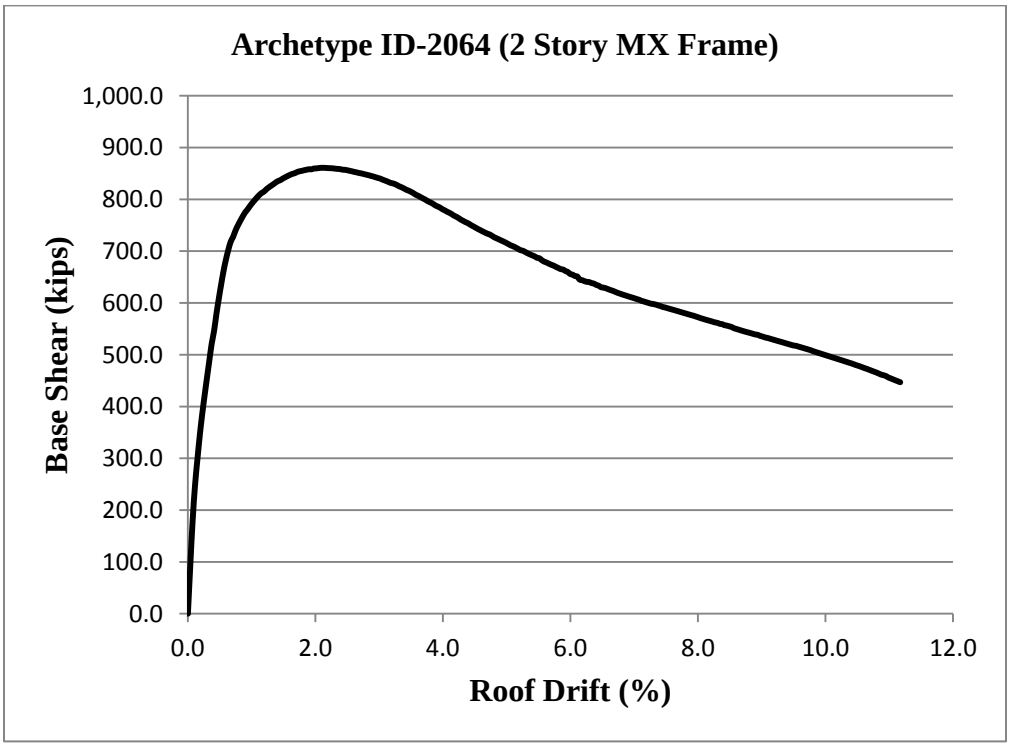

Figure 5-2 Pushover analysis result for model ID-2064 MX.

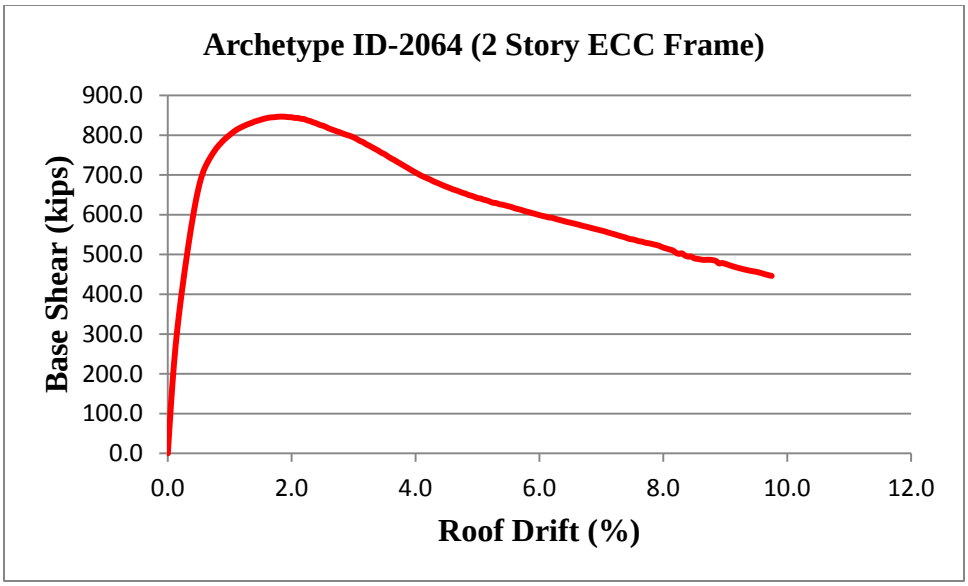

Figure 5-3 Pushover analysis result for model ID-2064 R/ECC.

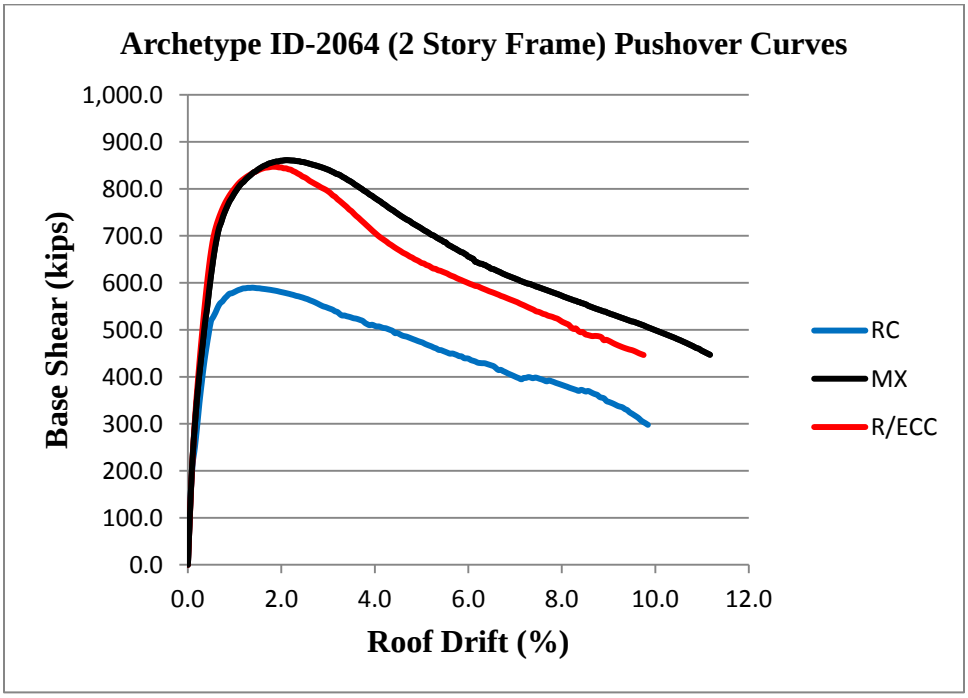

Figure 5-4 Pushover analysis results of ID-2064 frame.

Based on the static pushover analysis results, in most cases, MX frames have a higher maximum base shear values than R/ECC and RC frames. This behavior can be explained by the plastic hinge localization of the frames. While the plastic hinge localization of

both R/ECC and RC members occur at the member ends, it is formed at not only ECC part of the member but also formed at RC part of the member (Gencturk and Elnashai 2011) for MX frames. The calculated values of overstrength are used for overall derivation of system overstrength, and period based ductility values are used for adjustment of CMR based in the FEMA P695 methodology. Table 5-2 gives the computed values of overstrength, period based ductility and design base shear values of all archetype models.

5.4.1. Overstrength Calculation

After performing nonlinear static pushover analysis of the models, overstrength values are computed as the ratio of maximum base shear to design base shear. Calculated overstrength values for MX frames are 1.30 to 1.52 times higher than the RC models. This trend is also valid for the R/ECC models that the overstrength values for R/ECC frames are 1.25 to 1.52 times higher than the RC frames. Results are shown in Table 5-2 below.

5.4.2. Period Based Ductility Calculation

Period based ductility is the ratio of ultimate roof drift and effective yield displacement given by Equation (3-13). δ_u is the point where $0.8V_{max}$ is obtained and calculation of $\delta_{y,eff}$ is given by Equation (3-11). It is observed from the computed results shown in Table 5-2 that; RC frames have higher period based ductility values compared to both R/ECC and MX frames. In addition, the ductility values of the MX frames are slightly higher than those of the R/ECC frames. This trend is caused by material model definitions of "concrete" or "ECC". Furthermore, this can be also explained by the period

elongation of the reinforced concrete special moment frame structures before reaching collapse point (FEMA 2009).

5.5 Nonlinear Dynamic Analysis

As mentioned at Chapter 3, Section 5.2; nonlinear dynamic analysis is used to define CMR of each archetype building. All archetype model responses are evaluated after being subjected to the predefined "Far Field" ground motion record set. Each IDA curve shows the results from analysis of the frames up to collapse when subjected to an individual ground motion. Once all the analyses are completed; $\hat{S}_{CT}$ is calculated as the point where one half of records cause collapse. Approximately 400 nonlinear dynamic analyses are performed for each archetype depending on the scaling and collapse behavior. Figure 5-5, Figure 5-6 and Figure 5-7 show sample IDA results of archetype ID-1001, that is the two-story model of RC, MX and R/ECC frames.

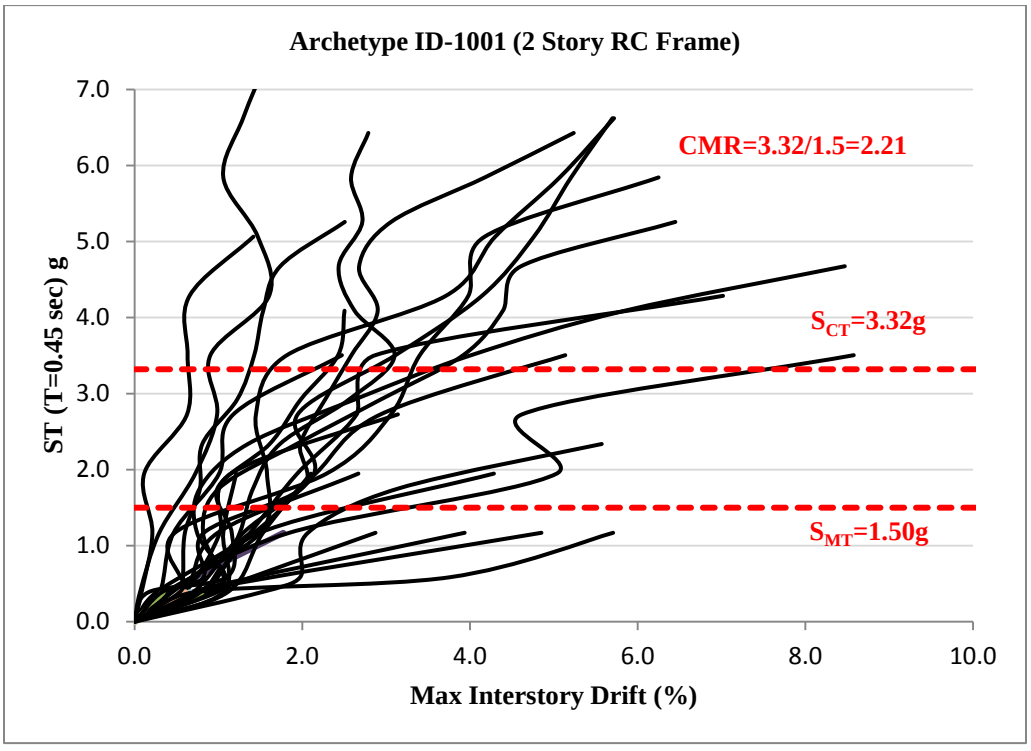

Figure 5-5 IDA result for ID-1001 two-story RC frame.

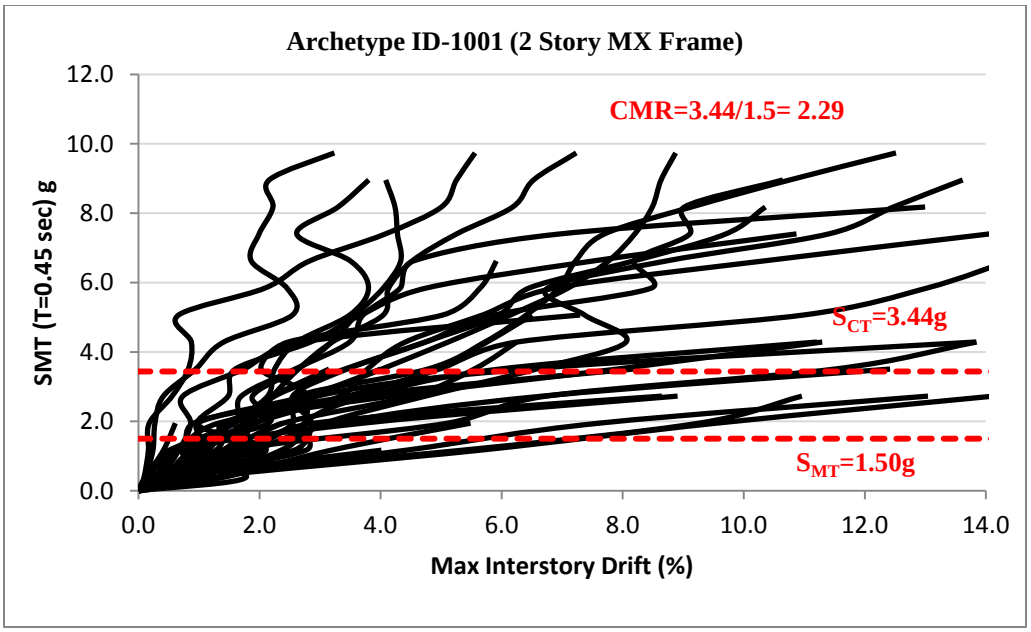

Figure 5-6 IDA result for ID-1001 two story MX frame.

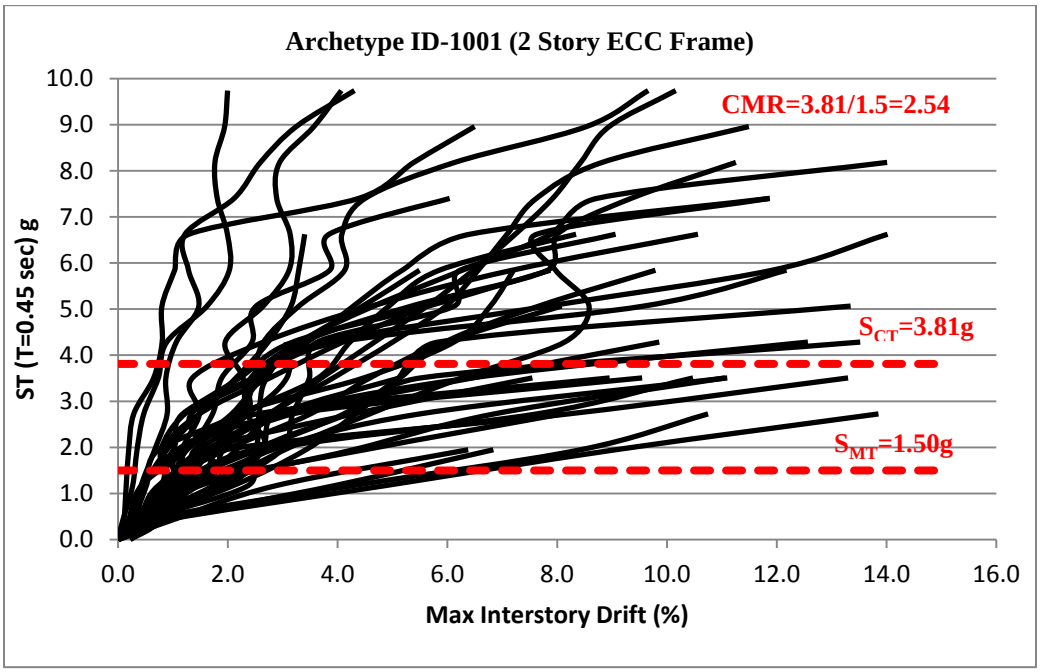

Figure 5-7 IDA result for ID-1001 two-story R/ECC frame.

The three figures given above provide a general idea about the IDA plots, collapse behavior mechanisms and CMR for the models. Calculated values of $\hat{S}_{CT}$ and CMR of RC, MX and R/ECC frames are shown in Table 5-2 below.

Table 5-2 Nonlinear Static and Nonlinear Dynamic Analysis Results.

Archetype ID		Design Configuration							Eigenvalue, Nonlinear Static, Nonlinear Dynamic Analysis Results				
		Stories	*Framing*	*SDC*	*R (Trial)*	*T (sec)*	*V/W*	S_{MT} *(T) (g)*	*Static* (Ω_0)	T_1 *(sec)*	S_{CT} *(T) (g)*	*CMR*	μ_T
2061	RC	1	S	Dmax	8	0.26	0.125	1.50	4.67	0.25	3.29	2.19	38.10
	MX	1	S		8	0.26	0.125	1.50	7.45	0.26	4.31	2.87	29.41
	R/ECC	1	S		8	0.26	0.125	1.50	7.27	0.27	4.10	2.73	28.57
2069	RC	1	P	Dmax	8	0.26	0.125	1.50	2.33	0.44	1.18	0.79	8.65
	MX	1	P		8	0.26	0.125	1.50	3.26	0.46	2.67	1.79	20.53
	R/ECC	1	P		8	0.26	0.125	1.50	3.21	0.47	2.56	1.70	17.60
1001	RC	2	S	Dmax	8	0.45	0.125	1.50	3.74	0.41	3.32	2.22	24.24
	MX	2	S		8	0.45	0.125	1.50	5.32	0.47	3.44	2.29	14.08
	R/ECC	2	S		8	0.45	0.125	1.50	5.33	0.52	3.81	2.54	13.39
2064	RC	2	P	Dmax	8	0.45	0.125	1.50	2.23	0.45	2.16	1.44	25.20
	MX	2	P		8	0.45	0.125	1.50	3.26	0.47	3.65	2.43	32.26
	R/ECC	2	P		8	0.45	0.125	1.50	3.21	0.48	3.24	2.16	27.58
1003	RC	4	P	Dmax	8	0.81	0.092	1.11	1.99	0.78	1.13	1.02	17.25
	MX	4	P		8	0.81	0.092	1.11	2.68	0.84	1.88	1.70	20.14
	R/ECC	4	P		8	0.81	0.092	1.11	2.56	0.86	1.52	1.37	13.82
1008	RC	4	S	Dmax	8	0.81	0.092	1.11	2.51	0.65	1.22	1.09	13.00
	MX	4	S		8	0.81	0.092	1.11	3.90	0.68	1.56	1.40	12.60
	R/ECC	4	S		8	0.81	0.092	1.11	3.80	0.70	1.54	1.39	13.20
1011	RC	8	P	Dmax	8	1.49	0.050	0.60	1.77	1.30	0.48	0.80	10.71
	MX	8	P		8	1.49	0.050	0.60	2.64	1.38	0.86	1.42	10.88
	R/ECC	8	P		8	1.49	0.050	0.60	2.52	1.41	0.47	0.79	6.29
1012	RC	8	S	Dmax	8	1.49	0.050	0.60	2.22	1.36	0.30	0.49	6.33
	MX	8	S		8	1.49	0.050	0.60	3.12	1.44	1.19	1.97	8.47
	R/ECC	8	S		8	1.49	0.050	0.60	3.07	1.48	1.12	1.86	8.11
1013	RC	12	P	Dmax	8	2.13	0.035	0.42	1.79	1.56	0.28	0.66	6.33
	MX	12	P		8	2.13	0.035	0.42	2.89	1.69	0.30	0.71	4.47
	R/ECC	12	P		8	2.13	0.035	0.42	2.66	1.73	0.29	0.68	4.33
1014	RC	12	S	Dmax	8	2.13	0.035	0.42	1.94	1.72	0.18	0.43	4.24
	MX	12	S		8	2.13	0.035	0.42	3.04	1.81	0.28	0.66	3.91
	R/ECC	12	S		8	2.13	0.035	0.42	2.94	1.84	0.21	0.50	3.57
1020	RC	20	P	Dmax	8	3.36	0.022	0.27	1.55	2.24	0.10	0.37	3.39
	MX	20	P		8	3.36	0.022	0.27	1.91	2.40	0.15	0.55	2.68
	R/ECC	20	P		8	3.36	0.022	0.27	2.28	2.45	0.21	0.80	3.46
1021	RC	20	S	Dmax	8	3.36	0.022	0.27	1.82	2.14	0.09	0.35	2.81
	MX	20	S		8	3.36	0.022	0.27	2.77	2.20	0.16	0.58	4.00
	R/ECC	20	S		8	3.36	0.022	0.27	2.98	2.29	0.21	0.79	3.10
1009	RC	30	P	Dmax	8	0.81	0.092	1.04	1.92	0.83	0.90	0.81	13.68
	MX	30	P		8	0.81	0.092	1.04	2.49	1.02	1.59	1.43	13.53
	R/ECC	30	P		8	0.81	0.092	1.04	2.39	1.10	1.66	1.50	12.04
1010	RC	30	S	Dmax	8	0.81	0.092	1.04	3.32	0.63	1.12	1.01	8.33
	MX	30	S		8	0.81	0.092	1.04	4.78	0.74	2.39	2.15	15.36
	R/ECC	30	S		8	0.81	0.092	1.04	4.55	0.80	1.61	1.45	8.59

Chapter 6 Derivation of Seismic Parameters

6.1 Adjusted Collapse Margin Ratio

ACMR is calculated using Equation (3-15) for all archetype models which is simply a multiplication of SSF and CMR. Table 3-6 shows the values of SSF for SDC D_{max}, which is a function of T and μ_T of the system. For values not shown in the Table 3-6, linear interpolation is done. Table 6-2, Table 6-3 and Table 6-4 show the computed values (ACMR) for the models.

6.1.1 Collapse Uncertainty

To quantify the acceptable CMR, total system uncertainty is calculated by Equation (3-11). The values of total uncertainty are given in Table 3-10 which accounts for uncertainties in modeling, data calibration, structural design, and earthquake records. Starting with a constant value of ground motion record uncertainty, which is 0.40; modeling uncertainty is decided as good, data for element calibration is determined good, and finally quality of structural system design requirements is determined as superior. Then Equation 3-13 is used to obtain the total system uncertainty, which is then in turn 0.50 and used for finding the acceptable CMR.

6.1.2 Acceptable Values of Adjusted Collapse Margin Ratio

The acceptable values of ACMR are chosen from the Table 6-1 based on the total collapse uncertainty and probability of collapse. Calculated total collapse uncertainty is 0.50 and ACMR values are 1.90 for average of performance groups and 1.52 for individual frames.

Table 6-1 Acceptable Values of Adjusted Collapse Margin Ratio (ACMR10% and ACMR20%).

Total System Collapse Uncertainty	Collapse Probability				
	5%	10% (ACMR 10%)	15%	20% (ACMR 20%)	25%
0.275	1.57	1.42	1.33	1.26	1.20
0.300	1.64	1.47	1.36	1.29	1.22
0.325	1.71	1.52	1.40	1.31	1.25
0.350	1.78	1.57	1.44	1.34	1.27
0.375	1.85	1.62	1.48	1.37	1.29
0.400	1.93	1.67	1.51	1.40	1.31
0.425	2.01	1.72	1.55	1.43	1.33
0.450	2.10	1.78	1.59	1.46	1.35
0.475	2.18	1.84	1.64	1.49	1.38
0.500	2.28	**1.90**	1.68	**1.52**	1.40
0.525	2.37	1.96	1.72	1.56	1.42
0.550	2.47	2.02	1.77	1.59	1.45
0.575	2.57	2.09	1.81	1.62	1.47
0.600	2.68	2.16	1.86	1.66	1.50
0.625	2.80	2.23	1.91	1.69	1.52
0.650	2.91	2.30	1.96	1.73	1.55
0.675	3.04	2.38	2.01	1.76	1.58
0.700	3.16	2.45	2.07	1.80	1.60
0.725	3.30	2.53	2.12	1.84	1.63
0.750	3.43	2.61	2.18	1.88	1.66
0.775	3.58	2.70	2.23	1.92	1.69
0.800	3.73	2.79	2.29	1.96	1.72
0.825	3.88	2.88	2.35	2.00	1.74
0.850	4.05	2.97	2.41	2.04	1.77
0.875	4.22	3.07	2.48	2.09	1.80
0.900	4.39	3.17	2.54	2.13	1.83
0.925	4.58	3.27	2.61	2.18	1.87
0.950	4.77	3.38	2.68	2.22	1.90

6.2 Evaluation of R factor

Performance groups are very important for the evaluation of *R*-factor. The trial values of *R* factor are assessed for each performance group. After finding the average value of

the performance groups, these values are used for verifying the trials values. Based on the results of FEMA P695 methodology followed in this thesis, trial *R* factor values are verified for RC, MX, and R/ECC models as shown in Table 6-2, Table 6-3, and Table 6-4.

Table 6-2 Summary of Collapse Margins and Comparison to Acceptance Criteria for RC Special Moment Frame Archetypes

Archetype ID		Design Configuration			Eigenvalue, Nonlinear Static, Nonlinear Dynamic Analysis Results					Acceptance Check	
		Stories	*Framing*	*SDC*	*Static (Ω)*	*μT*	*CMR*	*SSF*	*ACMR*	*Acceptable ACMR*	*Pass or Fail*
Performance Group No. PG-5 (Short Period, 20' Bay Width Configuration)											
PG 5	2069	1	P	Dmax	2.33	8.65	0.79	1.33	1.05	1.52	Fail
	2064	2	P		2.23	25.20	1.44	1.33	1.92	1.52	Pass
	----	3	P		2.11				1.68	1.52	Pass
Mean of Performance Group:					2.22				1.55	**1.90**	**Fail**
Performance Group No. PG-6 (Long Period, 20' Bay Width Configuration)											
PG 6	1003	4	P	Dmax	1.99	17.25	1.02	1.41	1.44	1.52	Fail
	1011	8	P		1.77	10.71	0.80	1.61	1.29	1.52	Fail
	1013	12	P		1.79	6.33	0.66	1.53	1.01	1.52	Fail
	1020	20	P		1.55	3.39	0.37	1.36	0.50	1.52	Fail
Mean of Performance Group:					1.78				1.06	**1.90**	**Fail**
Performance Group No. PG-1 (Short Period, 20' Bay Width Configuration)											
PG 1	2061	1	S	Dmax	4.67	38.10	2.19	1.33	2.91	1.52	Pass
	1001	2	S		3.74	24.24	2.22	1.33	2.95	1.52	Pass
	------	3	S		3.12				2.25	1.52	Pass
Mean of Performance Group:					3.84				2.70	**1.90**	**Pass**
Performance Group No. PG-3 (Long Period, 20' Bay Width Configuration)											
PG 3	1008	4	S	Dmax	2.51	13.00	1.09	1.41	1.54	1.52	Pass
	1012	8	S		2.22	6.33	0.49	1.53	0.75	1.52	Fail
	1014	12	S		1.94	4.24	0.43	1.42	0.61	1.52	Fail
	1021	20	S		1.82	2.81	0.35	1.30	0.46	1.52	Fail
Mean of Performance Group:					2.12				0.84	**1.90**	**Fail**
Performance Group No. PG-10 and PG-14 (30' Bay Width Configuration)											
PG 10	1009	4	P	Dmax	1.92	13.68	0.90	1.41	1.27	**1.52**	**Fail**
PG 14	1010	4	S	Dmax	3.32	8.33	1.12	1.41	1.58	**1.52**	**Pass**

Table 6-3 Summary of Collapse Margins and Comparison to Acceptance Criteria for MX Special Moment Frame Archetypes.

Archetype ID		Design Configuration			Eigenvalue, Nonlinear Static, Nonlinear Dynamic Analysis Results					Acceptance Check	
		Stories	*Framing*	*SDC*	*Static (Ω)*	*μT*	*CMR*	*SSF*	*ACMR*	*Acceptable ACMR*	*Pass or Fail*
Performance Group No. PG-5 (Short Period, 20' Bay Width Configuration)											
PG 5	2069	1	P	Dmax	3.26	20.53	1.79	1.33	2.38	1.52	Pass
	2064	2	P		3.26	32.26	2.43	1.33	3.23	1.52	Pass
	----	3	P		2.97				2.82	1.52	Pass
Mean of Performance Group:					3.15				2.81	**1.90**	**Pass**
Performance Group No. PG-6 (Long Period, 20' Bay Width Configuration)											
PG 6	1003	4	P	Dmax	2.68	20.14	1.70	1.41	2.40	1.52	Pass
	1011	8	P		2.64	10.88	1.42	1.61	2.29	1.52	Pass
	1013	12	P		2.89	4.47	0.71	1.43	1.02	1.52	Fail
	1020	20	P		1.91	2.68	0.51	1.29	0.66	1.52	Fail
Mean of Performance Group:					2.53				1.59	**1.90**	**Fail**
Performance Group No. PG-1 (Short Period, 20' Bay Width Configuration)											
PG 1	2061	1	S	Dmax	7.45	29.41	2.87	1.33	3.81	1.52	Pass
	1001	2	S		5.32	14.08	2.29	1.33	3.05	1.52	Pass
	------	3	S		4.61				2.51	1.52	Pass
Mean of Performance Group:					5.79				3.12	**1.90**	**Pass**
Performance Group No. PG-3 (Long Period, 20' Bay Width Configuration)											
PG 3	1008	4	S	Dmax	3.90	12.60	1.40	1.41	1.97	1.52	Pass
	1012	8	S		3.12	8.47	1.97	1.61	1.56	1.52	Pass
	1014	12	S		3.04	3.91	0.66	1.39	0.92	1.52	Fail
	1021	20	S		2.77	4.00	0.51	1.40	0.71	1.52	Fail
Mean of Performance Group:					3.21				1.29	**1.90**	**Fail**
Performance Group No. PG-10 and PG-14 (30' Bay Width Configuration)											
PG 10	1009	4	P	Dmax	2.49	13.53	1.43	1.41	2.02	**1.52**	**Pass**
PG 14	1010	4	S	Dmax	4.78	15.36	2.15	1.41	3.03	**1.52**	**Pass**

Table 6-4 Summary of Collapse Margins and Comparison to Acceptance Criteria for R/ECC Special Moment Frame Archetypes.

Archetype ID		Design Configuration			Eigenvalue, Nonlinear Static, Nonlinear Dynamic Analysis Results					Acceptance Check	
		Stories	*Framing*	*SDC*	*Static (Ω)*	*μT*	*CMR*	*SSF*	*ACMR*	*Acceptable ACMR*	*Pass or Fail*
Performance Group No. PG-5 (Short Period, 20' Bay Width Configuration)											
PG 5	2069	1	P	Dmax	3.21	17.6	1.70	1.33	2.26	1.52	Pass
	2064	2	P		3.21	27.58	2.16	1.33	2.87	1.52	Pass
	----	3	P		2.89				2.40	1.52	Pass
Mean of Performance Group:					3.07				2.51	**1.90**	**Pass**
Performance Group No. PG-6 (Long Period, 20' Bay Width Configuration)											
PG 6	1003	4	P	Dmax	2.56	13.82	1.37	1.41	1.93	1.52	Pass
	1011	8	P		2.52	6.29	0.79	1.53	1.21	1.52	Fail
	1013	12	P		2.66	4.33	0.68	1.42	0.97	1.52	Fail
	1020	20	P		2.28	3.46	0.80	1.36	1.09	1.52	Fail
Mean of Performance Group:					2.51				1.30	**1.90**	**Fail**
Performance Group No. PG-1 (Short Period, 20' Bay Width Configuration)											
PG 1	2061	1	S	Dmax	7.27	28.57	2.73	1.33	3.63	1.52	Pass
	1001	2	S		5.33	13.39	2.54	1.33	3.38	1.52	Pass
	------	3	S		4.58				2.67	1.52	Pass
Mean of Performance Group:					5.73				3.23	**1.90**	**Pass**
Performance Group No. PG-3 (Long Period, 20' Bay Width Configuration)											
PG 3	1008	4	S	Dmax	3.80	13.20	1.39	1.41	1.96	1.52	Pass
	1012	8	S		3.07	8.11	1.86	1.61	2.99	1.52	Pass
	1014	12	S		2.94	3.57	0.50	1.36	0.68	1.52	Fail
	1021	20	S		2.98	3.10	0.79	1.33	1.05	1.52	Fail
Mean of Performance Group:					3.21				1.67	**1.90**	**Fail**
Performance Group No. PG-10 and PG-14 (30' Bay Width Configuration)											
PG 10	1009	4	P	Dmax	2.39	12.04	1.50	1.41	2.11	**1.52**	**Pass**
PG 14	1010	4	S	Dmax	4.55	8.59	1.45	1.41	2.04	**1.52**	**Pass**

6.3 Evaluation of Overstrength Factor

System overstrength factors are evaluated separately for RC, MX, and R/ECC frames. Table 6-5 shows that perimeter frame performance groups PG-5 and PG-6 have lower overstrength values than the space frame performance groups PG-1 and PG-3 overstrength values. Additionally, overstrength values of long period structures are lower than the overstrength values of short period archetypes. It is also observed that the four-story 9144 mm bay width design archetypes overstrength values are higher than the four-story 6096 mm bay width design archetypes overstrength values. The results are parallel with FEMA P695 methodology results for RC frames. These findings are also valid for both MX and R/ECC models.

Due to enhanced properties of ECC, both MX and R/ECC model overstrength values are higher than the RC model values. MX model values are 1.3 to 1.52 times and R/ECC model values are 1.25 to 1.52 times higher than the RC model values.

Table 6-5 Average overstrength results of performance groups.

Performance Groups	Framing Types	Bay Width	Period Domain	Frame Types		
				RC	MX	R/ECC
PG-5	P	6096 mm	Short	2.22	3.15	3.07
PG-6	P	6096 mm	Long	1.78	2.53	2.51
PG-1	S	6096 mm	Short	3.84	5.79	5.73
PG-3	S	6096 mm	Long	2.12	3.21	3.21
PG-10	P	9144 mm	Long	1.92	2.49	2.39
PG-14	S	9144 mm	Long	3.32	4.78	4.55

6.4 Evaluation of Deflection Amplification Factor

FEMA P695 methodology defined C_d is derived based on the acceptable value of the R and damping factors. The equation given by the FEMA P695 methodology is

$$C_d = \frac{R}{B_I}, \tag{6-1}$$

where C_d is the deflection amplification factor, R is the response modification factor and BI is a numerical coefficient for damping, which depends on the effective damping (β_I) and period of the system. β_I is one of the critical parameters for calculating C_d. According to ASCE 7-05, the damping of structures should be determined "based on the material type, configuration, and behavior of the structure and nonstructural components responding dynamically at or just below yield of the seismic force-resisting system" (ASCE 2006). Following the code definition, β_I of the RC, MX, and R/ECC models are calculated below the yield point by means of reverse cyclic pushover analysis. Figure 6-1 illustrates the idealized energy dissipation area just below the yield point and the damping factor is calculated as

$$\xi = \frac{1}{2\pi}\frac{E_D}{E_{So}}, \tag{6-2}$$

where E_D is the energy loss and, E_{So} is the maximum strain energy. Reverse cyclic analysis is performed for the models and calculated values of β_I are given in Table 6.2 below.

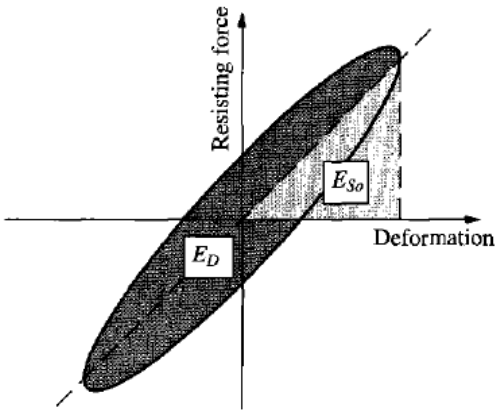

Figure 6-1 Illustration of energy loss of system in a cycle and maximum strain energy (Chopra 2007)

Table 6-6 Calculated effective damping values of frames

Archetype ID	Story Number	RC Frame	MX Frame	R/ECC Frame
2061	1	6.36	13.21	15.02
2069	1	7.78	10.21	11.98
1001	2	6.25	10.88	14.79
2064	2	7.00	11.49	13.61
1003	4	4.88	9.76	11.45
1008	4	7.09	11.06	13.00
1011	8	6.41	13.53	12.64
1012	8	5.52	11.39	12.46
1013	12	7.86	15.31	12.40
1014	12	6.66	12.33	12.65
1020	20	5.80	9.97	12.28
1021	20	6.26	9.66	11.66
1009	4	5.79	9.86	12.51
1010	4	6.12	10.65	13.74
Mean value		6.40	9.80	11.20

The FEMA P695 methodology assumed a critical value of β_I equal to 5% and the corresponding B_I is given by the Table 18.6-1 of ASCE 7-05 (2006) as 1.00 and therefore for most systems C_d is equal to the *R*-factor according to Equation (6-1). The analysis results here shows that β_I for RC frames is close to 5% as defined in the ASCE 7-05 (2006). On the other hand, the damping factors of RC frames and MX and R/ECC frames are around 9% and 11%, respectively. Based on these findings, B_I value is considered equal to 1.06 for RC frames, 1.19 for MX frames and 1.24 for R/ECC frames.

Chapter 7 Conclusions

7.1 Summary

In this thesis, seismic design parameters; namely, response modification, system overstrength and displacement amplification factors are derived for reinforced concrete moment resisting frames based on the procedure outlined in FEMA P695 (FEMA 2009). Two different buildings designs are considered. These models are named R/ECC and MX. In R/ECC, the concrete is entirely replaced with HPFRC. Today, HPFRC can be as expensive as 4-5 times the cost of conventional concrete depending on the selection of the mixture materials and fibers. Therefore, in the MX, to address the cost issue, only the plastic hinge regions are built from HPFRC while reinforced concrete is used for the rest of the buildings. Additionally, to validate the model design and quality, and to compare the results with FEMA P695, RC models are also evaluated. 14 different frames are modeled each of the RC, MX and R/ECC models. The seismic design factors are quantified using the current code concepts, with the help of incremental dynamic analyses and finally by means of risk assessment techniques.

7.2 Observations and Conclusions

Based on results of the nonlinear static and dynamic analysis, R/ECC and MX frame types result with higher margin when compared to a conventional RC frame. For the RC frames, the calculated average overstrength values for high seismic 6096 mm bay width performance groups are 2.22 and 1.78 for perimeter frames (PG-5 and PG-6), 3.84 and 2.12 for space frames (PG-1 and PG-3). For MX frames, the calculated average overstrength values are 3.15 and 2.53 for perimeter frames (PG-5 and PG-6), 5.79 and 3.21 for space frames (PG-1 and PG-3). These R/ECC frame overstrength values are

close to MX frames overstrength values. Perimeter frame performance groups (PG-5 and PG-6) computed values are 3.07 and 2.51, space frame performance groups (PG-1 and PG-3) values are 5.73 and 3.21. Based on these results, it is observed that MX frames static analysis responses are very close to R/ECC frames response and both have higher overstrength compared to RC frames as expected.

The average ACMRs for each performance groups are also in favor of frames using ECC. For the perimeter frame performance groups (PG-5 and PG-6) ACMRs are 1.55 and 1.06 for RC, 2.81 and 1.59 for MX and, 2.51 and 1.30 for R/ECC frames. For the space frame performance groups (PG-1 and PG-3) ACMRs are 2.70 and 0.84 for RC, 3.12 and 1.29 for MX and, 3.23 and 1.67 for R/ECC frames. These results based on the FEMA P695 methodology show that the seismic performance of the frames using ECC is substantially improved compared to the conventional concrete frame design. In other words, the margins of safety against collapse for MX and R/ECC frames are higher compared to RC frames. Moreover, this trend is also valid for high seismic 9144 mm bay width performance groups.

Some of the RC, MX, and R/ECC performance groups ACMR values did not meet the FEMA P695 acceptable ACMR values. This is caused by the differences between the ultimate roof displacements (δ_u) values of the frames defined in Haselton and Deierlein (2008) and calculated values in this study. Table 7-1 gives the calculated ultimate displacement and period based ductility values from static pushover analysis as found here and those used values in FEMA P695 (FEMA 2009). It is seen from Table 7-1 that several of the frames yield a lower ultimate displacement value in this study which results in lower CMR values as a result of how the non-simulated collapse modes are treated in

this study as compared to that in Haselton and Deierlein (2008). In addition, there are significant differences in modeling approaches between the two studies. Here, a distributed plasticity models with fiber-based beam-column elements are used; while, Haselton and Deierlein (2008) use a lumped plasticity approach with rotational springs a the beam-column joints. The differences in the CMR values are also attributed to the differences in the modeling approach. These findings were important to illustrate the sensitivity of the assessments using FEMA P695 methodology to the modeling approach.

Table 7-1 Comparison of ultimate displacement ,$\delta_{u,}$ and period based ductility ,$\mu_{T,}$ values.

Model ID		**FEMA P695**		**FEMA P695**
	δ_u	δ_u	μ_T	μ_T
2069	2.68	7.7	8.65	14
2064	5.04	6.7	25.20	19.6
1003	4.14	3.8	17.25	10.9
1011	2.25	2.3	10.71	9.8
1013	1.71	2.6	6.33	11.4
1020	1.22	1.8	3.39	5.6
2061	8	7.7	38.10	16.1
1001	8	8.5	24.24	14
1008	4.03	4.7	13.00	11.3
1012	1.71	2.8	6.33	7.5
1014	1.23	2.2	4.24	7.7
1021	1.18	2.3	2.81	5.7
1009	3.42	5	13.68	13.4
1010	3.25	5.6	8.33	13.2

The FEMA P695 methodology suggests that the system overstrength value (Ω_0) should not be selected less than the largest average value of calculated overstrength value. The largest average value for RC, MX, and R/ECC frames are 3.84, 5.79 and 5.73, respectively.

The C_d values are calculated based on Equation (6-1). For RC frames, FEMA P695 (FEMA 2009) recommends that the C_d values are equal to the *R*-factors. Results of cyclic pushover analysis for RC frames show that the average inherent damping is equal to % 6 and C_d is equal to 0.94**R*. This results match with the FEMA P695 suggestion that the inherent damping is equal to % 5 for RC frames and C_d equal to *R*. On the other hand, the results of the cyclic pushover analysis for inherent damping calculation shoved that the C_d value can be taken 0.84**R* and 0.81**R* for MX frames and R/ECC frames respectively.

The results obtained here favor MX and R/ECC frames over conventional RC frames with higher overstrength factors and larger margins against collapse. Based on these results, the *R* value of 8 can be further increased for MX and R/ECC frames. In other words, a higher level of safety is achieved against collapse for these frames.

7.3 Recommendations for Future Research

One of the limitations of this study is the lack of large scale experiments for the verification of material properties, designs and final behavior of the HPFRC models. Further verification of these results is needed through large-scale experiments. Moreover, a detailed study on the effect of the panel region at the beam-column joints is needed. The results in thesis are proposed as a basis for further research on seismic design of HPFRC and multi-material buildings.

References

ACI. 2002. Recommendations for Design of Beam-Column Connections in Monolithic Reinforced Concrete Structures, American Concrete Institute (ACI 352R-02).

ACI. 2005. Building Code Requirements for Structural Concrete and Commentary, American Concrete Institute (ACI 318M-05).

ACI. 2008. Building code requirements for structural concrete (ACI 318-08) and commentary. Farmington Hills, Mich.: American Concrete Institute.

Alath, Sailaja, and Sashi K Kunnath. 1995. Modeling inelastic shear deformation in RC beam-column joints. Paper read at Engineering Mechanics (1995).

Altoontash, Arash, and Gregory G. Deierlein. 2004. *Simulation and damage models for performance assessment of reinforced concrete beam-column joints*. Stanford University, 2004.

Anderson, James C, and William H Townsend. 1977. "Models for RC frames with degrading stiffness." *Journal of the Structural Division* no. 103 (12):2361-2376.

ASCE. 2006. Minimum design loads for buildings and other structures, American Society of Civil Engineers. (ASCE/SEI 7-05).

ASCE. 2007. Seismic Rehabilitation of Existing Buildings, American Society of Civil Engineers. (ASCE/SEI 41-06).

ASCE. 2013. Minimum design loads for buildings and other structures (ASCE/SEI 7-10). American Society of Civil Engineers.

ATC. 1978. *Tentative Provisions for the Development of Seismic Regulations for Buildings*: National Bureau of Standards.

ATC. 1995. *Structural Response Modification Factors, (ATC-19)*. Redwood City, California: Applied Technology Council.

ATC. 2009. *Quantification of building seismic performance factors*. Applied Technology Council.

Baker, Jack W, and C Allin Cornell. 2006. "Spectral shape, epsilon and record selection." *Earthquake Engineering & Structural Dynamics* no. 35 (9):1077-1095.

Biddah, Ashraf, and A Ghobarah. 1999. "Modelling of shear deformation and bond slip in reinforced concrete joints." *Structural Engineering and Mechanics* no. 7 (4):413-432.

Billington, Sarah L, and JK Yoon. 2004. "Cyclic response of unbonded posttensioned precast columns with ductile fiber-reinforced concrete." *Journal of Bridge Engineering* no. 9 (4):353-363.

Blume, John A, Nathan M Newmark, and Leo H Corning. 1961. *Design of Multistory Reinforced Concrete Buildings for Earthqueake Motions*: Portland Cement Assoc.

Brooke, Nicholas, Les Megget, Richard Fenwick, and Jason Ingham. 2004. "Bond strength of reinforced concrete-beam column joints incorporating 500 Mpa reinforcement." *SESOC Journal* no. 17 (2):37-46.

Canbolat, B Afsin, Gustavo J Parra-Montesinos, and James K Wight. 2005. "Experimental study on seismic behavior of high-performance fiber-reinforced cement composite coupling beams." *ACI Structural Journal-American Concrete Institute* no. 102 (1):159-166.

Chopra, Anil K. 2007. Dynamics of structures: theory and applications to earthquake engineering. Prentice-Hall.

Clyde, Chandra, Chris P Pantelides, and Lawrence D Reaveley. 2000. *Performance-based evaluation of exterior reinforced concrete building joints for seismic excitation*: Pacific Earthquake Engineering Research Center, College of Engineering, University of California, Berkeley.

Council, International Code. 2006. International Building Code (IBC). Falls Church VA.

Durrani, Ahmad Jan, and James K. Wight. 1982.*Experimental and analytical study of internal beam to column connections subjected to reversed cyclic loading*.

El-Metwally, SE, and WF Chen. 1988. "Moment-rotation modeling of reinforced concrete beam-column connections." *ACI Structural Journal* no. 85 (4).

Elmorsi, Mostafa, M Reza Kianoush, and WK Tso. 2000. "Modeling bond-slip deformations in reinforced concrete beam-column joints." *Canadian Journal of Civil Engineering* no. 27 (3):490-505.

Elnashai, Amr, and Luigi Di Sarno. 2008. *Fundamentals of earthquake engineering*: Wiley. com.

Elnashai, AS, and AM Mwafy. 2002. "Overstrength and force reduction factors of multistorey reinforced-concrete buildings." *The Structural Design of Tall Buildings* no. 11 (5):329-351.

Elnashai, AS, V Papanikolaou, and D Lee. 2010. "Zeus-NL-A System for Inelastic Analysis of Structures-User Manual." *Mid-America Earthquake (MAE) Center, Department of Civil and Environmental Engineering, University of Illinois at Urbana-Champaign, Urbana*.

Endoh, Yoshio, Takehiro Kamura, S Otani, and H Aoyama. 1991. "Behavior of R/C beamcolumn connections using light-weight concrete." *Trans. Jpn. Concr. Inst* no. 13:319-326.

FEMA. 2003. "NEHRP recommended provisions for seismic regulations for new buildings and other structures." *Report FEMA-450 (Provisions), Federal Emergency Management Agency (FEMA), Washington*.

FEMA. 2009. "Quantification of Building Seismic Performance Factors. (FEMA P695)." *Federal Emergency Management Agency, Washington DC*.

Filiatrault, Andre, Karim Ladicani, and Bruno Massicotte. 1994. "Seismic performance of code-designed fiber reinforced concrete joints." *ACI structural journal* no. 91 (5).

Filiatrault, Andre, Sylvain Pineau, and Jules Houde. 1995. "Seismic behavior of steel-fiber reinforced concrete interior beam-column joints." *ACI Structural journal* no. 92 (5).

Fischer, Gregor, and Victor C Li. 2002. "Effect of matrix ductility on deformation behavior of steel-reinforced ECC flexural members under reversed cyclic loading conditions." *ACI Structural Journal* no. 99 (6):781-790.

Fukuyama, Hiroshi, Yukihiro Sato, Victor C Li, Yasuhiro Matsuzaki, and Hirozo Mihashi. 2000. "Ductile engineered cementitious composite elements for seismic structural applications." *CD Proceedings of the 12 WCEE, Paper* no. 1672.

Gebman, Michael. 2001. *Application of steel fiber reinforced concrete in seismic beam-column joints*, San Diego State University.

Gencturk, Bora, and Amr S Elnashai. 2013. "Numerical modeling and analysis of ECC structures." *Materials and Structures* no. 46 (4):663-682.

Gencturk, Bora Esref, and AS Elnashai. 2011. *Multi-objective optimal seismic design of buildings using advanced engineering materials*. Vol. 73.

Giberson, Melborne F. 1969. "Two nonlinear beams with definitions of ductility." *Journal of the Structural Division*.

Haselton, CB, and JW Baker. 2006. Ground motion intensity measures for collapse capacity prediction: Choice of optimal spectral period and effect of spectral shape. Paper read at 8th National Conference on Earthquake Engineering.

Haselton, Curt B., and Gregory G. Deierlein. 2008. *Assessing seismic collapse safety of modern reinforced concrete moment-frame buildings*, *PEER report,*. Berkeley, Calif.: Pacific Earthquake Engineering Research Center.

Henager, CH. 1977. "Steel Fibrous-Ductile Concrete Joint for Seismic-Resistant Structures." *ACI Special Publication* no. 53.

Higashi, Yoichi, and Yoshimasa Ohwada. 1969. *Failing Behaviors of Reinforced Concrete Beam-column Connection Subjected to Lateral Load*.

Ibarra, Luis F., and Helmut Krawinkler. 2005. *Global collapse of frame structures under seismic excitations*, *PEER report*. Berkeley, Calif.: Pacific Earthquake Engineering Research Center.

IBC. 1961. Uniform building code. International Code Council

IBC. 2000. *International building code 2000*. International Code Council

IBC. 2003. International Building Code. International Code Council.

IBC. 2009. International Building Code. International Code Council.

Jiuru, Tang, Hu Chaobin, Yang Kaijian, and Yan Yongcheng. 1992. "Seismic behavior and shear strength of framed joint using steel-fiber reinforced concrete." *Journal of Structural Engineering* no. 118 (2):341-358.

Kaku, T, and H Asakusa. 1991. "Bond and anchorage of bars in reinforced concrete beam-column joints." *ACI Special Publication* no. 123.

Kanda, T, S Watanabe, and Victor C Li. 1998. "Application of pseudo strain hardening cementitious composites to shear resistant structural elements." *AEDIFICATIO Publishers, Fracture Mechanics of Concrete Structures* no. 3:1477-1490.

Katzensteiner, B, S Mindess, A Filiatrault, and ND Nathan. 1992. Use of steel fibre concrete in seismic design. Paper read at RILEM PROCEEDINGS.

Kavitha, D, and SR Damodarasamy. 2009. Basics of Structural Dynamics and Aseismic Design.: New Delhi: Prentice-Hall Of India Pvt. Ltd.

Leon, Roberto T. 1990. "Shear strength and hysteretic behavior of interior beam-column joints." *ACI Structural Journal* no. 87 (1).

Leyendecker, Edgar V, R Joe Hunt, Arthur D Frankel, and Kenneth S Rukstales. 2000. "Development of maximum considered earthquake ground motion maps." *Earthquake Spectra* no. 16 (1):21-40.

Li, Victor C. 1992a. Performance driven design of fiber reinforced cementitious composites. Paper read at RILEM Proceedings.

Li, Victor C. 1992b. "Postcrack scaling relations for fiber reinforced cementitious composites." *Journal of Materials in Civil Engineering* no. 4 (1):41-57.

Li, Victor C, and Christopher KY Leung. 1992. "Steady-state and multiple cracking of short random fiber composites." *Journal of Engineering Mechanics* no. 118 (11):2246-2264.

Li, Victor C, and Hwai-Chung Wu. 1992. "Conditions for pseudo strain-hardening in fiber reinforced brittle matrix composites." *Journal of Applied Mechanics Review* no. 45 (8):390-398.

Lowes, Laura N, and Arash Altoontash. 2003. "Modeling reinforced-concrete beam-column joints subjected to cyclic loading." *Journal of Structural Engineering* no. 129 (12):1686-1697.

Mander, John B, Michael JN Priestley, and R Park. 1988. "Theoretical stress-strain model for confined concrete." *Journal of structural engineering* no. 114 (8):1804-1826.

Martínez-Rueda, J Enrique, and AS Elnashai. 1997. "Confined concrete model under cyclic load." *Materials and Structures* no. 30 (3):139-147.

Meinheit, Donald Fred, and James Otis Jirsa. 1977. *The shear strength of reinforced concrete beam-column joints*: Department of Civil Engineering, Structures Research Laboratory, the University of Texas at Austin.

Noguchi, H, and T Kashiwazaki. 1992. Experimental studies on shear performances of RC interior column-beam joints with high-strength materials. Paper read at 10 th World Conference on Earthquake Engineering.

Oka, Koji, and Hitoshi Shiohara. 1992. Tests on high-strength concrete interior beam–column joint sub-assemblages. Paper read at Proc., 10th World Conf. on Earthquake Engineering.

Osteraas, John David, and Helmut Krawinkler. 1990. *Strength and ductility considerations in seismic design*: Stanford University.

Otani, Shunsuke. 1974. "Inelastic analysis of R/C frame structures." *Journal of the Structural Division* no. 100 (7):1433-1449.

Otani, Shunsuke, Yutaka Kobayashi, and Hiroyuki Aoyama. 1984. *Reinforced concrete interior beam-column joints under simulated earthquake loading*: University of Tokyo, Department of Architecture.

Pan, J L, and F Yuan. 2013. "Seismic Behaviors of ECC/Concrete composite beam-column joints under reversed cyclic loading." *VIII International Conference on Fracture Mechanics of Concrete and Concrete Structures*.

Park, R, and Dai Ruitong. 1988. "Ductility of doubly reinforced concrete beam sections." *ACI structural Journal* no. 85 (2).

Parra-Montesinos, Gustavo, and James K Wight. 2000. "Seismic response of exterior RC column-to-steel beam connections." *Journal of structural engineering* no. 126 (10):1113-1121.

PEER. 2006. "NGA Database, Pacific Earthquake Engineering Research Center." *University of California, Berkeley, USA, http://peer.berkeley.edu/nga*.

Ramberg, Walter, and William R Osgood. 1943. *Description of stress-strain curves by three parameters*: National advisory committee for aeronautics (NACA).

SEAOC. 1959. *Recommended Lateral Force Requirements and Commentary*. California: Structural Engineers Association of California.

Shannag, M Jamal, Nabeela Abu-Dyya, and Ghazi Abu-Farsakh. 2005. "Lateral load response of high performance fiber reinforced concrete beam–column joints." *Construction and Building Materials* no. 19 (7):500-508.

Sharpe, RL, S Freeman, and B Safavi. 1982. "An investigation of the correlation between earthquake ground motion and building performance." *Appl. Tech. Counc. Rept*.

Shin, Myoungsu, and James M LaFave. 2004. "Modeling of cyclic joint shear deformation contributions in RC beam-column connections to overall frame behavior." *Structural Engineering and Mechanics* no. 18 (5):645-670.

Shiohara, Hitoshi. 2004. Quadruple flexural resistance in R/C beam-column joints. Paper read at 13 th World Conference on Earthquake Engineering.

Somma, G. "RC and FRC Beam-Column Joints under Seismic Loading–Shear Strength."

Somma, G. 2011. "RC and FRC Beam-Column Joints under Seismic Loading–Shear Strength." *International Journal of Earth Sciences and Engineering* no. 4:1078-1081.

Uang, Chia-Ming. 1991. "Establishing R (or R w) and C d factors for building seismic provisions." *Journal of Structural Engineering* no. 117 (1):19-28.

Uang, Chia-Ming, and Ahmed Maarouf. 1994. "Deflection amplification factor for seismic design provisions." *Journal of Structural Engineering* no. 120 (8):2423-2436.

Vamvatsikos, Dimitrios, and C. Allin Cornell. 2002. Incremental dynamic analysis. *Earthquake Engineering & Structural Dynamics*, 31 (3): 491-514.

Walker, Steven G. 2001. *Seismic performance of existing reinforced concrete beam-column joints*. M s c e, University of Washington.

Youssef, M, and A Ghobarah. 2001. "Modelling of RC beam-column joints and structural walls." *Journal of Earthquake Engineering* no. 5 (01):93-111.

Zareian, Farzin. 2006. *Simplified performance-based earthquake engineering*. Thesis (PhD), Stanford University, 2006.

APPENDIX

A. Nonlinear Static Pushover Analysis Results

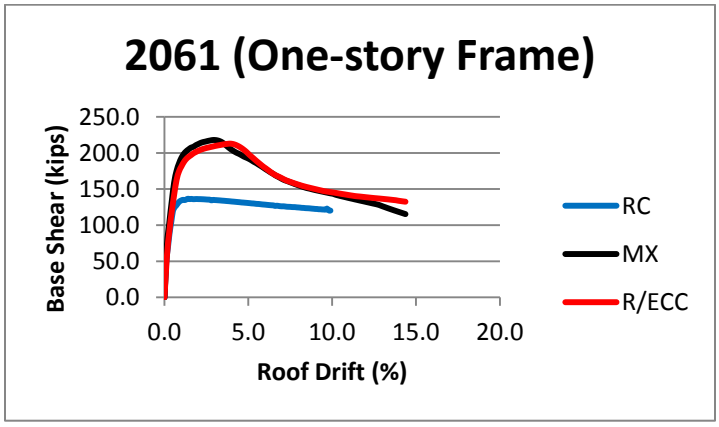

Figure A-1 Static pushover analysis results of ID-2061.

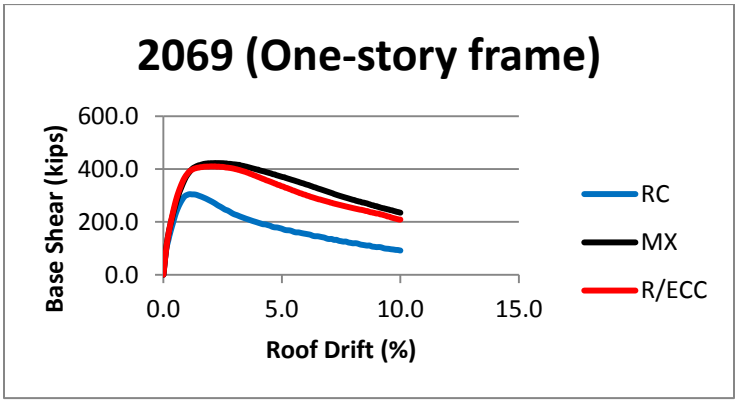

Figure A-2 Static pushover analysis results of ID-2069.

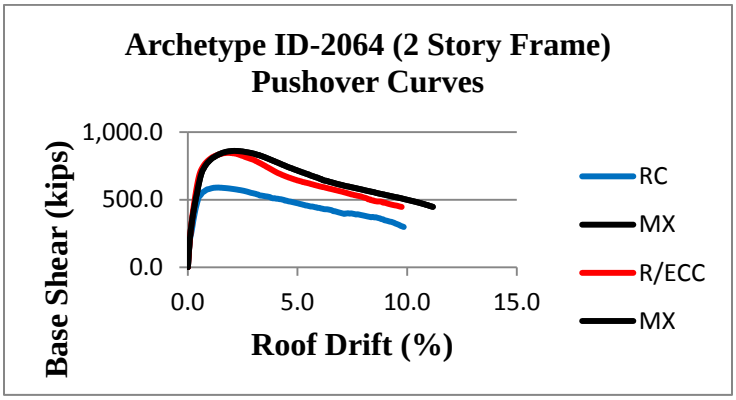

Figure A-3 Static pushover analysis results of ID-2064.

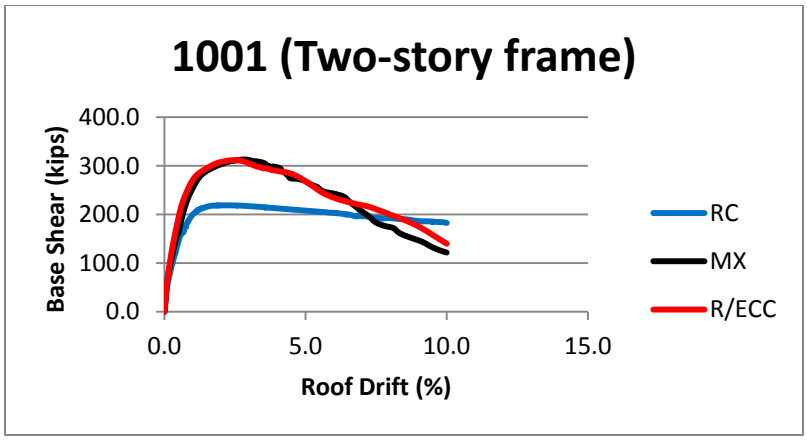

Figure A-4 Static pushover analysis results of ID-1001.

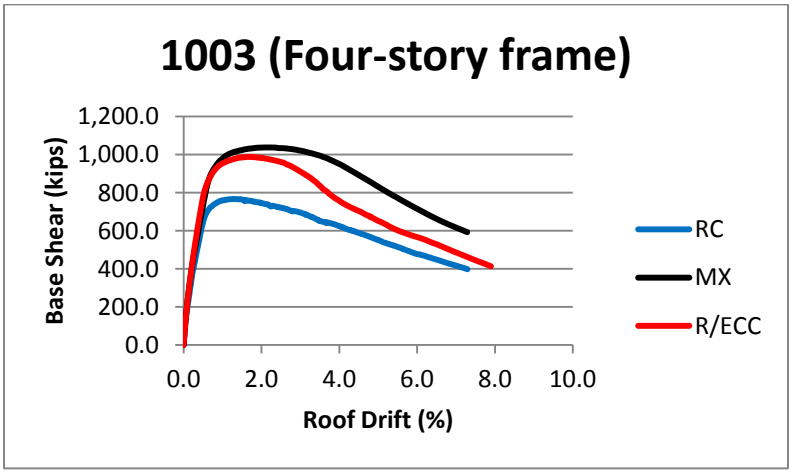

Figure A-5 Static pushover analysis results of ID-1003.

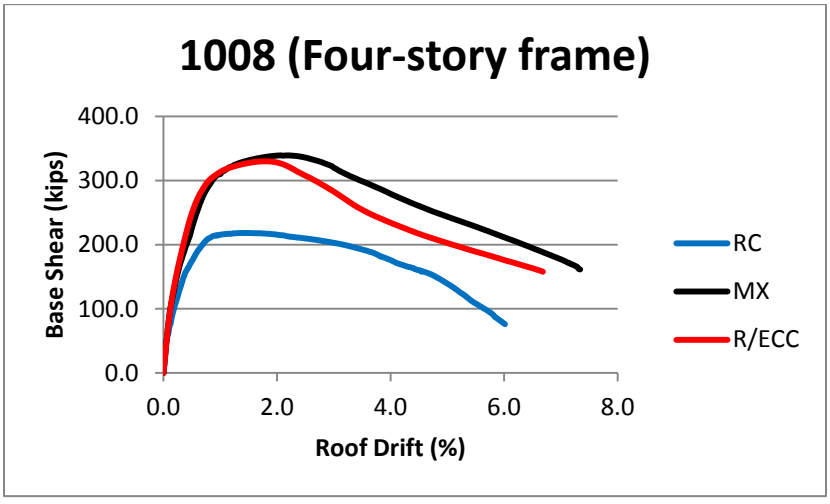

Figure A-6 Static pushover analysis results of ID-1008.

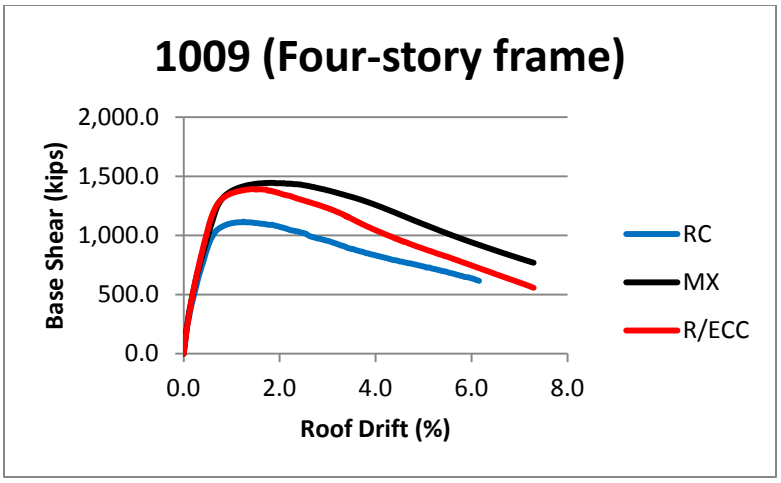

Figure A-7 Static pushover analysis results of ID-1009.

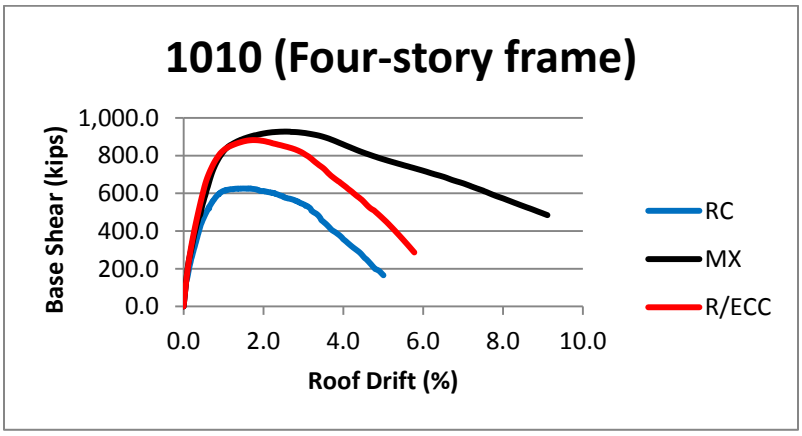

Figure A-8 Static pushover analysis results of ID-1010.

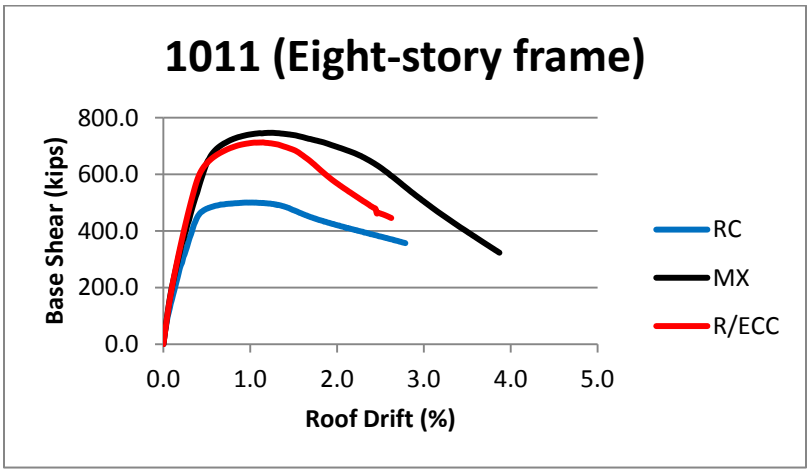

Figure A-9 Static pushover analysis results of ID-1011.

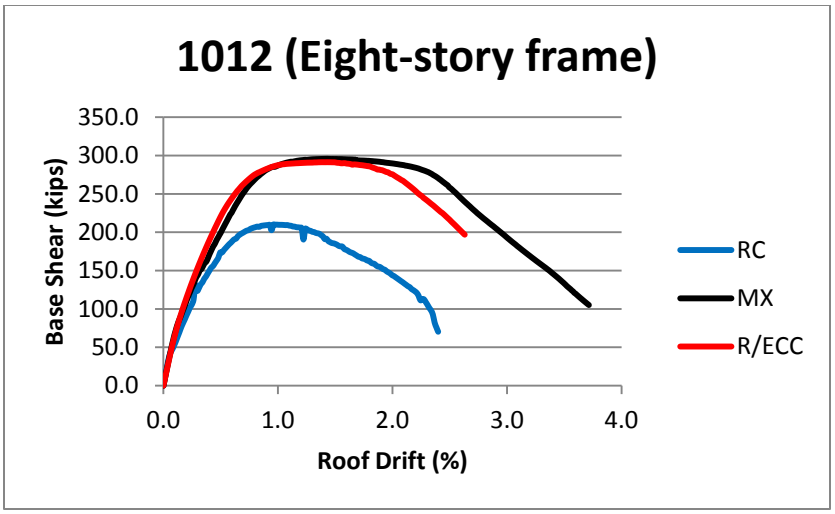

Figure A-10 Static pushover analysis results of ID-1012.

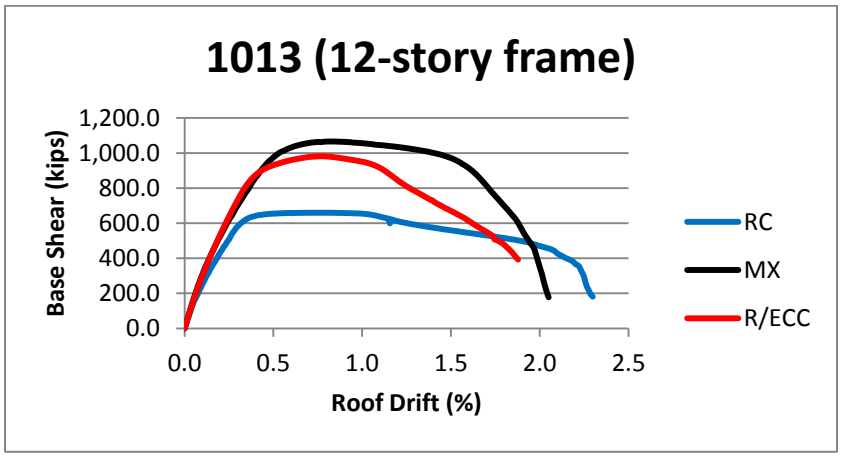

Figure A-11 Static pushover analysis results of ID-1013.

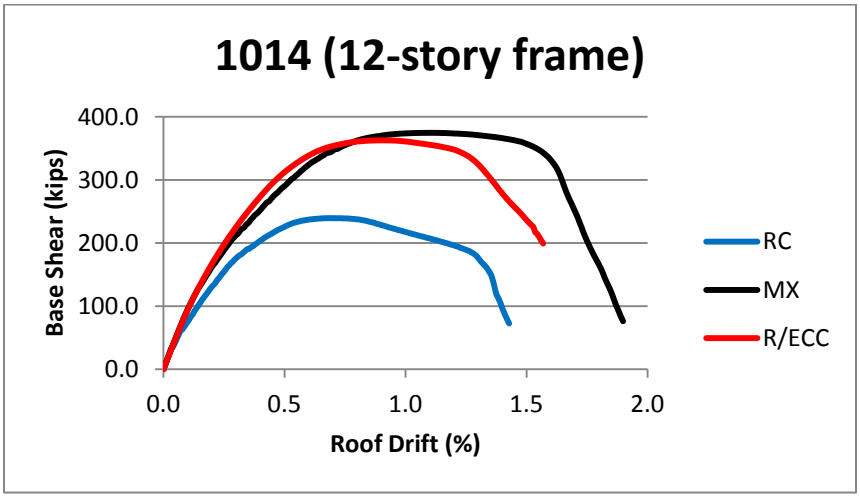

Figure A-12 Static pushover analysis results of ID-1014.

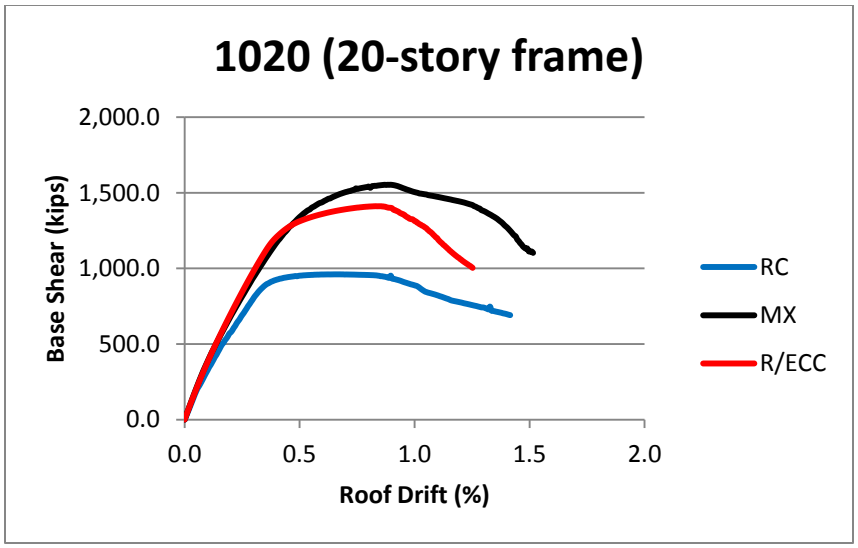

Figure A-13 Static pushover analysis results of ID-1020.

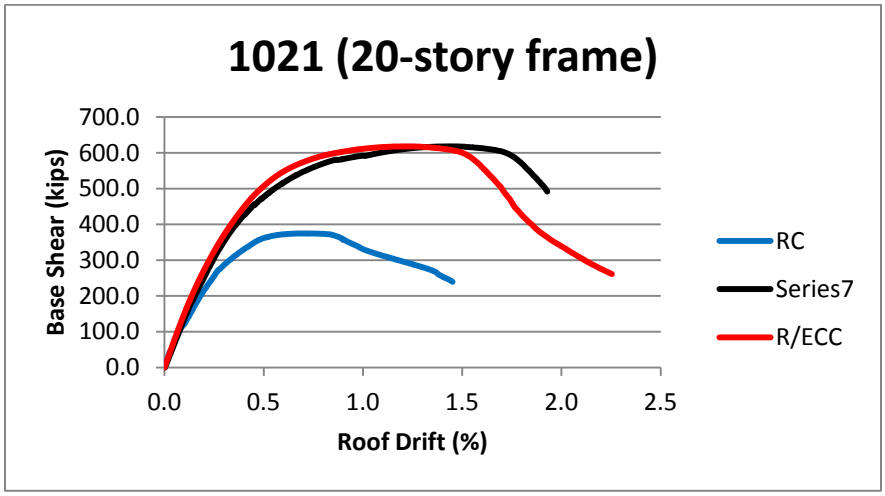

Figure A-14 Static pushover analysis results of ID-1021.